Conceptualising carbon cycling pathways across different land-use types based on rates and ages of soil-respired CO_2

Luisa I. Minich[1, 2], Dylan Geissbühler[3], Stefan Tobler[1], Annegret Udke[1,5], Alexander S. Brunmayr[2], Margaux Moreno Duborgel[1,2], Ciriaco McMackin[4], Lukas Wacker[5], Philip Gautschi[5], Negar Haghipour[2,5], Markus Egli[4], Ansgar Kahmen[6], Jens Leifeld[7], Timothy I. Eglinton[2], Frank Hagedorn[1]

[1] Forest Soils and Biogeochemistry, Swiss Federal Institute for Forest, Snow and Landscape Research (WSL), Birmensdorf, Switzerland
[2] Biogeoscience, Department of Earth and Planetary Sciences, ETH Zurich, Zurich, Switzerland
[3] Laboratory for the Analysis of Radiocarbon with AMS, Department of Chemistry, Biochemistry and Pharmaceutical Sciences, University of Bern, Bern, Switzerland
[4] Geochronology, Department of Geography, University of Zurich, Zurich, Switzerland
[5] Laboratory for Ion Beam Physics, Department of Physics, ETH Zurich, Zurich, Switzerland
[6] Physiological Plant Ecology, Department of Environmental Sciences, University of Basel, Basel, Switzerland
[7] Climate and Agriculture Group, Agroscope, Reckenholz, Switzerland

Correspondence to: Luisa I. Minich (luisa.minich@gmail.com)

Abstract. Soil carbon dioxide (CO_2) efflux constitutes a major carbon (C) transfer from terrestrial ecosystems to the atmosphere, driven by numerous metabolic and allocation processes in the plant-soil system. Land use affects key components of C cycling pathways through vegetation type, C allocation, abiotic conditions, and management impacts on soil organic matter (SOM). However, systematic comparisons of these pathways among land uses remain scarce. In two contrasting seasons, we measured respiration rates and C isotopic signatures (^{14}C, ^{13}C) of *in situ* soil-respired CO_2 and its autotrophic and heterotrophic sources derived from incubations at 16 sites across Switzerland, covering temperate and alpine grasslands, forests, croplands, and managed peatlands. Our findings revealed significant differences in the rates, ages, and sources of soil-respired CO_2 between land-use types, reflecting variations in C cycling dynamics. We propose that respiration rates and ages of soil-respired CO_2 serve as comprehensive indicators to categorize C cycling into:

1. **High-throughput systems** (temperate grasslands) where high respiration rates of young (< 10 years) CO_2 reveal rapid C cycling.
2. **Temperature-constrained retarding systems** (alpine grasslands) where the respiration of decadal- to centennial-old CO_2 reveals slow C cycling mainly due to cooler climatic conditions.
3. **Input-constrained retarding systems** (forests) where decadal-old CO_2 reflects a delayed C transfer of assimilates back to the atmosphere through soil respiration.
4. **C-depleted systems** (croplands) where reduced C inputs and tillage lead to C depletion and to respiratory losses of centennial-old C.
5. **Hotspots of C release** (managed peatlands) where ancient C is lost through respiration due to disturbances in natural C cycling by drainage.

Our results suggest that the relationship between rates and ages of soil-respired CO_2 can serve as a robust indicator of C retention and loss along the trajectory from natural to anthropogenically disturbed systems on a global scale.

Graphical abstract

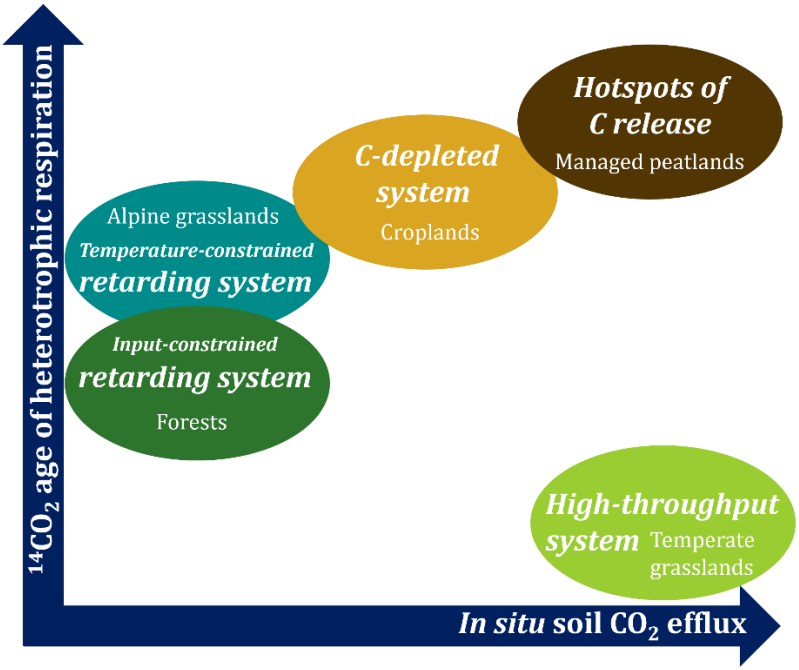

1 Introduction

Soil carbon dioxide (CO_2) efflux is one of the largest carbon (C) fluxes between terrestrial ecosystems and the atmosphere with CO_2 release from soils exceeding fossil fuel CO_2 emissions (IPCC, 2021; Nissan et al., 2023). Soil CO_2 fluxes (i.e., soil respiration) originate from root activity related to the metabolic processing and allocation of C in plants (i.e., autotrophic respiration), as well as the mineralization of various soil organic matter (SOM) compounds by microorganisms (i.e., heterotrophic respiration) (Kuzyakov, 2006; Trumbore, 2006). In this study, we refer to rhizosphere respiration as all respiratory processes within the rhizosphere, including autotrophic respiration by root activity as well as heterotrophic respiration related to the consumption of root exudates by mycorrhizal fungi and other rhizosphere microorganisms (Hanson et al., 2000; Trumbore, 2006). Relative source contributions are essential to determine the pathways and velocity of belowground C cycling. A dominance of autotrophic respiration indicates high gross primary productivity (GPP) (Schulze et al., 2009) or rapid cycling of plant assimilates through the plant-soil system (Diao et al., 2022; Fuchslueger et al., 2016; Gao et al., 2021), largely bypassing storage in soil. In contrast, a higher contribution of heterotrophic respiration indicates that a large fraction of C enters the soils as plant detritus, which is then respired during degradation and transformation processes.

Land use impacts soil respiration and its source contributions through various factors such as vegetation type, root density, nutrient input, and management practices, altering soil structure and C cycling pathways within the plant-soil system (e.g., Oertel et al., 2016; Rong et al., 2015; Schaufler et al., 2010; Xiao et al., 2021). In Europe, grasslands have the highest soil

respiration rates, followed by wetlands, croplands, and forests (Schaufler et al., 2010). Grasslands are among the most productive land-use types in Europe, due to their high GPP and net primary productivity (NPP) (Schulze et al., 2009), high belowground C allocation (Fuchslueger et al., 2016; Hagedorn & Joos, 2014; R. Wang et al., 2021), dense rooting system, and rapid fine root turnover (Leifeld et al., 2015; Solly et al., 2013) which together accelerate C cycling through the plant-soil system. In forests, aboveground C inputs are greater than in agricultural systems, where aboveground biomass is regularly removed (Hiltbrunner et al., 2013; Keel et al., 2019). These inputs – particularly woody debris and conifer litter – decompose slowly and lead to the formation of organic layers (Hiltbrunner et al., 2013; Tangarife-Escobar et al., 2024; Zanella et al., 2011), reducing the rate of C release back to the atmosphere. In arable land used for crop production, tillage and biomass removal disturb natural C cycling and induces the depletion of SOC stocks (Keel et al., 2019), especially in managed C-rich peatlands (Leifeld et al., 2005). Swiss peatlands, which store large amounts of C on a per area basis, have been intensively used for agriculture over the past century. Conversion of the majority (82 %) of these peatlands to other land uses has led to severe degradation, causing high C losses (Wüst-Galley et al., 2020).

Despite their relevance in the global C cycle, soil CO_2 effluxes and their sources remain one of the greatest sources of uncertainty in global C budgets and in understanding climate feedbacks (Konings et al., 2019; Li et al., 2016; Tharammal et al., 2019). One reason is the methodological challenge of quantifying the sources of soil-respired CO_2 under natural conditions. Common approaches rely on destructive techniques such as trenching or girdling (e.g., Diao et al., 2022; Shi et al., 2022; Wunderlich & Borken, 2012), are constrained by their short-term nature such as ^{13}C pulse-labelling (Gao et al., 2021; R. Wang et al., 2021), or by their differences in natural abundance $\delta^{13}C$ signatures which do not allow for distinction of autotrophic sources from the decomposition of young SOC compounds (e.g., Diao et al., 2022; Millard et al., 2010). Radiocarbon (^{14}C) analysis provides a powerful tool to determine the age of respired CO_2, which in turn corresponds to the mean transit time of C – the time C spends in the terrestrial ecosystem from photosynthesis until respiration (Bolin & Rodhe, 1973; Eriksson, 1971; Sierra et al., 2017). Nuclear weapons testing in the 1950s and 1960s led to nearly a doubling in the amount of atmospheric $^{14}CO_2$ in the Northern hemisphere (commonly known as the "bomb-spike"), inadvertently serving as a large-scale tracer experiment. Since then, atmospheric $^{14}CO_2$ levels have been diluted due to the emission of ^{14}C-free fossil fuels (Schuur et al., 2016) and the incorporation of $^{14}CO_2$ into the ocean and terrestrial ecosystems. The ^{14}C bomb-spike can be used to investigate C incorporation and cycling in terrestrial ecosystems on decadal time scales (Graven et al., 2024). In combination with stable carbon (^{13}C) isotope analysis, ^{14}C measurements of CO_2 from *in situ* soil respiration as well as autotrophic and heterotrophic respiration from incubations provide a non-destructive approach to determine source contributions to total soil respiration based on their distinct isotopic signatures (e.g., Borken et al., 2006; Schuur & Trumbore, 2006). Soil incubation experiments under controlled conditions can further inform about SOC decomposability, the SOC fraction that is potentially readily available for microbial decomposition, by relating rates of heterotrophic respiration to SOC contents of the soil samples (Schädel et al., 2019). High SOC decomposability suggests a large fraction of readily available organic matter, whereas low SOC decomposability indicates greater persistence and stability of SOC and/or advanced decomposition of more labile SOM.

Radiocarbon and stable isotopic approaches have been used to investigate the age and source contributions of respired CO_2 in natural ecosystems (e.g., Hicks Pries et al., 2013; Phillips et al., 2013; Schuur & Trumbore, 2006; Wunderlich & Borken, 2012). However, these techniques have not yet been used in agro-ecosystems such as intensely managed grasslands, croplands, and drained peatlands. In our study, we investigated the magnitude, velocity, and pathways of C cycling across five dominant land-use types in Switzerland which span a gradient from natural to intensely managed and disturbed ecosystems: grasslands (temperate and alpine), forests, croplands, and managed peatlands. We measured soil respiration rates and C isotopic signatures ($\Delta^{14}CO_2$ and $\delta^{13}CO_2$) of total soil respiration and its sources and used Bayesian mixing models to determine the age and source contribution for each land-use type. Our main goals were (i) to assess how the flux rates, ages, and source contributions of soil-respired CO_2 vary across dominant land-use types in Switzerland, (ii) to determine how these variables change seasonally, and (iii) to develop a conceptual framework to describe how CO_2 age and soil respiration rates can be used to identify and characterise C cycling pathways in various land-use types, in order to detect SOC losses, and to assess the vulnerability of C cycling in these systems to land-use and climate change.

We hypothesized that CO_2 age and soil respiration rates under different land-use types are driven by the interplay of vegetation (productivity, belowground allocation, litter quality), climate, soil physicochemical properties, and management practices. Specifically, we expected that (i) temperate grasslands predominantly respire young, few year old CO_2 at a high rate due to high belowground C allocation and high autotrophic contributions driven by abundant fine root biomass; (ii) alpine grasslands respire decadal-old CO_2 because colder climate slows down C turnover in the plant-soil system; (iii) forests respire decadal-old CO_2 at lower rates than grasslands, due to slower litter decomposition and a higher proportion of heterotrophic respiration, (iv) croplands release decadal- up to centennial-old CO_2 at low rates, because of reduced C inputs and tillage, which deplete soils in labile C and leave behind persistent, older SOC; and finally (v) managed peatlands release the oldest up to millennial-old CO_2 at high rates, driven by the decomposition of preserved C and high heterotrophic respiration following drainage.

2 Materials and methods

2.1 Study sites

We sampled soil-respired CO_2, roots, and soil from 16 sites of five dominant land-use types in Switzerland: grasslands (temperate and alpine), forests, intensively managed croplands, and managed peatlands (drained and used as croplands). Land-use types were chosen based on established classifications following the Land use, land-use change and forestry (LULUCF) categories defined by the IPCC (IPCC, 2021; IPCC, 2003), with an additional distinction between temperate and alpine grasslands to account for climatic differences. The 16 sites vary in their physicochemical soil properties, span a climatic as well as elevational gradient from 393 to 2630 meters above sea level (a.s.l.) and encompass four of Switzerland's five ecoregions (Table 1, Fig. S1). Site properties are typical for the respective land-use type across Switzerland. Generally, croplands and managed peatlands are found under relatively similar environmental conditions of the Swiss Plateau, whereas grasslands and forests occur across a broader range of climate conditions. We deliberately chose sites from Swiss monitoring

programs to capture variability in climate and soil properties allowing us to test the robustness of land-use type effects on rates, ages, and source contribution of respired CO_2. Grasslands were either used as meadows (Chamau, Muldain) in the lowlands, including mowing and manure application, or as pasture (Jaun, alpine grasslands), including grazing. The three cropland sites resemble each other in crop type (July/August: maize, March: wheat; Table 1) and management practices, and are part of long-
125 term field trials of the Swiss Federal Research Institute Agroscope, Switzerland, established 35 and 49 years ago (for Changins: e.g., Maltas et al., 2018; for Altwi, Reckenholz: e.g., Hirte et al., 2021). As part of the Swiss Plateau near settlements, the sites had been used as grassland, orchards and vineyards until the 19th century and had then been converted to croplands before they were used for the long-term cropping trials (Oberholzer et al., 2014). All cropland sites were treated with mineral fertilizer according to the Swiss fertilization guidelines (Flisch et al., 2009) and regularly ploughed before sowing to a soil depth of
130 approximately 25 cm. The managed peatlands were drained in the second half of the 19th century and have been used for crop production ever since (Leifeld et al., 2011). Crop types differ between each peatland site and season, with most of the cultivated crops being vegetables (Table 1).

Table 1: Site specific information on climate, soil type, and vegetation/crop type.

Land-use type	Location				Climate		Soil properties			Soil type (WRB classification)	Vegetation / Crop type	
	Site name	Lat	Lon	Elevation [m a.s.l]	MAP [mm]	MAT [°C]	pH (0-10 cm)	SOC (0-10 cm) [%]	N (0-10cm) [%]		July/August	March
Grassland												
Temperate	Chamau	47.2102	8.4104	393	1134	9.9	6.3	2.9	0.3	Cambisol/Gleysol	Italian ryegrass, white clover	
	Vaz Muldain	46.6903	9.5196	1200	1040	4.9	7.0	7.1	0.9	Gleyic Fluvisol	mixed grasses	
	Jaun	46.6114	7.2727	1500	1712	6.0	5.2	5.8	0.6	Eutric Cambisol	mixed grasses	
Alpine	Flüelapass	46.7433	9.9632	2320	1622[a)]	0.4[a)]	3.5	6.3	0.5	-	mixed grasses	
	Büelenhorn	46.6791	9.7793	2340	1622[a)]	-0.1[a)]	6.6	12	1.5	-	mixed grasses	
	Radönt	46.7118	9.9387	2340	1622[a)]	0.4[a)]	3.7	15.0	1.0	-	mixed grasses	
	Schwarzhorn	46.7335	9.9530	2630	1622[a)]	-1.2[a)]	4.0	7.6	0.6	-	mixed grasses	
Forest												
	Beatenberg	46.7003	7.7625	1511	1725	4.7	3.1	6.6	0.3	Podzol	Norway Spruce	
	Pfynwald	46.3031	7.6121	615	575	10.6	6.2	11.9	0.5	Pararendzina	Scots pine	
	Hölstein	47.4381	7.7769	550	1009[b)]	9.0[b)]	5.2	6.2	0.5	-	European beech, Norway Spruce	
Cropland												
	Reckenholz	47.4307	8.5220	440	1050	9.4	5.5	2.4	0.3	Eutric Gleysol	summer maize	winter wheat
	Altwi	47.4386	8.5255	493	1050	9.4	7.4	1.4	0.2	Calcaric Cambisol	summer maize	winter wheat
	Changins	46.3820	6.2389	446	994	10.7	7.1	0.9	0.1	Calcaric Cambisol	summer maize	winter wheat
Managed peatland												
	Lindergut	46.9797	7.0983	430	1030[c)]	10.7[c)]	7.0	11.5	0.9	Histosol	mixed grasses	
	Rimmerzmatte	47.0117	7.0772	432	1030[c)]	10.7[c)]	7.0	10.4	0.8	Histosol	onion	cover grass
	Underi Site	47.0245	7.2044	438	1030[c)]	10.7[c)]	7.1	17.5	1.5	Histosol	summer maize	

*[a)] Alpine sites: **MAP** from MeteoSwiss station Weissflühhorn (2690 Hm), **MAT** from IMIS stations (FLU2 for Flüelapass and Radönt, DAV2 for Büelenhorn, ZNZ2 for Schwarzhorn)*
*[b)] Hölstein: **MAP and MAT** from MeteoSwiss station Basel-Binningen*
*[c)] Managed peatlands: **MAP** from MeteoSwiss station Aarberg, **MAT** from MeteoSwiss station Neuchatêl*

2.2 In situ CO_2 flux measurements and gas sampling

We measured rates and sampled CO_2 from total soil respiration *in situ* at all sites during two sampling campaigns: one in July/August 2023 and another in March 2024. These months were selected to capture the greatest variability in the soil environmental conditions while avoiding snow cover and melt. Severe climatic conditions precluded a sampling in March at the three alpine grassland sites.

At each of the 16 sites, we inserted three opaque cylindrical PVC frames (Ø = 30 cm; height = 15-25 cm; volume ~ 15 L) approximately 3-5 cm deep into the soil and 1-2 m apart to account for soil heterogeneity. Chambers were installed 1-2 weeks before sampling to allow soil respiration to re-equilibrate after installation disturbance. To exclude the contribution of above-ground plant respiration, vegetation inside the chamber was clipped at installation and before sampling if plants had regrown. We measured CO_2 fluxes for each of the three chambers via a flow-through system using a LI-COR gas analyser (LI-8100A, LI-COR®). CO_2 fluxes were calculated as the rate of change in concentration over time in the chamber headspace using a linear approach while correcting for air pressure and mean chamber temperature using Gay-Lussac's ideal gas law (Butterbach-Bahl et al., 2011). Chamber closure times during flux measurements were 3-10 minutes. After flux measurements, chambers were flushed with CO_2-free air five times the chamber volume (ca. 75 L) and sealed until CO_2 levels reached ~ 1000 ppm for subsequent ^{14}C analysis. Air from all three chambers was composited into a 2 L air bag (Cali-5-Bond, Calibrated Instruments, LLC, USA). A detailed description of the sampling procedure is presented in Supplement S1 and Fig. S2. For ^{13}C analysis, we sampled gas from each of the three chambers separately, transferring headspace air into pre-evacuated 12 mL Exetainer® vials using a 60 mL syringe. The lack of spatial and temporal replicates for each site is a consequence of the limited capacity of ^{14}C measurements. In March, we repeated the CO_2 sampling and subsequent isotopic analysis for three spatial replicates at the forest sites Hölstein and Pfynwald. Results of the spatial replication are presented in Supplement S6, Fig. S9, and Table S6.

For atmospheric background $^{14}CO_2$ measurements, ambient air (~ 20 cm above the soil surface) was sampled into 5 L air bags (Cali-5-Bond, Calibrated Instruments, LLC, USA). Soil environmental conditions were monitored before and after gas sampling. Ambient air temperature was measured at the height of the chamber (~ 15 cm above soil surface). Soil temperature and volumetric water content (VWC) were monitored at 10 cm soil depth using a thermometer and HH2 moisture meter (Delta-T Devices Ltd), respectively.

2.3 Soil sampling and analysis

During the July/August sampling campaign, we sampled soil at the centre of each PVC frame after the gas sampling was completed. Soil cores were taken with a Humax corer (Ø = 5 cm) down to 52 cm soil depth. Sampling was continued as deep as possible (maximum depth = 90 cm) using a soil auger (Ø = 5 cm). Soil samples were stored at 2 °C until further processing. We split the mineral soil samples from the three soil cores into depth intervals of 0-5, 5-10, 10-20, 20-40, and 40-90 cm for all sites. At the forest sites, we additionally sampled organic layers (i.e., litter (L), fermented horizon (F), and humified horizon (H; only present at Beatenberg)). Alpine grassland sites were sampled separately by excavating soil profiles and taking volume-

proportional samples for the pre-defined depth intervals. Volumes were estimated by simple measurements of the excavated areas and samples were weighed and sieved to 4 mm in the field prior to processing in the laboratory.

For further analysis, we pooled and homogenized the soil of the three cores and corresponding depths to yield one composite sample per depth and site. In order to measure the released CO_2 by heterotrophic respiration during incubation, we removed the roots and skeleton by sieving subsample at 4 mm. We acknowledge that sieving can disrupt soil structure and expose otherwise protected SOC but was necessary to remove roots contributing to the CO_2 release. However, we tried to limit aggregate disruption by careful sieving at 4 mm compared to the standard 2mm-sieving. Subsamples were dried at 40 °C, sieved them to 2 mm, and ground to fine powder using a ball mill (MM2000, Retsch).

Gravimetric water content (GWC) was determined for each soil sample by drying a subsample of 6-10 g of fresh soil at 105 °C for 48 h. Bulk density was obtained by calculating the dry soil weight for each depth layer. Fine soil mass in each layer was determined by subtraction of the weight of the skeleton (> 2 mm). The volume of the skeleton was calculated by assuming a density of 2.65 g cm^{-3} for stones (Walthert et al., 2002).

2.4 Root and soil incubations

We determined isotopic signatures of autotrophic and heterotrophic endmembers by conducting short-term root and soil incubations. Root incubations were prepared during the sampling campaigns *in situ*. We excavated fine roots (< 2 mm), including mycorrhizae within the chambers at 0-10 cm soil depth after the gas sampling. We carefully removed soil particles and rinsed the roots in an ultrapure water bath while keeping the root system as intact as possible. Roots from all three chambers were combined into one composite sample and incubated instantly, as the $\delta^{13}C$ value of excised roots can slightly change after a few minutes (Midwood et al., 2006). We placed approximately 10 g of fresh roots into 2 L glass bottles that were wrapped in aluminium foil to exclude light. We immediately flushed the glass bottles with CO_2-free air until all ambient air was removed. Roots were incubated overnight at approximately 22 °C, followed by gas sampling into a 2 L air bag using a flow-through system. A detailed description of the sampling procedure from incubations is presented in Supplement S2. Gas for ^{13}C analysis was sampled thereafter as described for *in situ* soil respiration.

Soil incubations were performed for each depth layer using the same procedure as for root incubations. Depending on the depth layer and their SOC contents, we incubated soil corresponding to dry soil weights between 30 and 250 g. Soils were incubated at 22 °C and field soil moisture levels. Depending on the respiration rates, the incubation time varied between one day and four weeks. We calculated basal respiration rates for each soil incubation by integrating the entire incubation period. Basal respiration was used as a proxy for SOC decomposability by relating it to the SOC content.

2.5 Isotopic analysis of gas samples

The $^{13}CO_2$ contents of all gas samples were measured by an isotope-ratio mass spectrometer (IRMS Gas-Bench II coupled with a Delta-V Advanced IRMS, Thermo GmbH, Germany) at the Swiss Federal Research Institute of Forest, Snow and Landscape WSL. Graphitization and ^{14}C measurements were performed at the Laboratory of Ion Beam Physics, ETH Zurich, Switzerland.

For ^{14}C analysis, gas samples were graphitized using an Air Loading Facility (ALF; Gautschi, 2017) coupled to an Automated Graphitization Equipment (AGE3, ETH Zurich, Switzerland; Wacker, Němec, et al., 2010) with an integrated zeolite trap to adsorb CO_2 from the sampling bag. The $^{14}CO_2$ contents of all gas samples were measured using a MIni radioCArbon DAting System (MICADAS, ETH Zurich, Switzerland; Synal et al., 2007) or a Low Energy AMS (LEA, ETH Zurich & IonPlus AG, Switzerland; Ramsperger et al., 2024). Measurement uncertainties were < 2 ‰. For data evaluation, the standard Oxalic Acid II (Mann, 1983) and blank material from the ^{14}C-free phthalic anhydride (PhA) were measured alongside the samples and evaluated with the BATS software (Wacker, Christl, et al., 2010).

2.6 Isotopic analysis of bulk soil

Bulk soil samples were analysed for total and organic C, and $\delta^{13}C$ by dry combustion with an automated elemental analyser – continuous flow isotope ratio mass spectrometer (Euro-EA 3000, HEKAtech GmbH, Germany, interfaced with a Delta-V Advanced IRMS, Thermo GmbH, Germany). Measurements were corrected against primary reference materials (VPDB and AIR). Measurement uncertainties were < 0.3 ‰. Samples with $\delta^{13}C$ values exceeding -25 ‰, which suggest a potential contribution of inorganic C, were additionally analysed after fumigation with 37 % HCl to remove inorganic C (Walthert et al., 2010).

For ^{14}C analysis, potential inorganic C was removed for all samples by fumigation with 37 % HCl (Komada et al., 2008; Walthert et al., 2010). Samples were acidified for 72 h at 60 °C and neutralized with NaOH pellets (72 h, 60 °C). All glassware was combusted at 550 °C for 5 h prior to use. ^{14}C measurements in SOC of bulk soil were performed on a MICADAS featuring a gas ion source and coupled to an Elemental Analyser (EA vario MICRO cube, Elementar, Germany; Ruff et al., 2010) at the Laboratory of Ion Beam Physics, ETH Zurich, Switzerland. Measurement uncertainties were 6-8 ‰.

Comparisons of isotopic signatures from heterotrophically respired CO_2 and SOC revealed possible contributions of carbonate weathering to CO_2 for some sites and depths. We assumed contributions of carbonate weathering in cases where $\Delta^{14}C$ signatures indicated CO_2 age > SOC age and/or in cases where $\delta^{13}CO_2 > \delta^{13}C$ of SOC (except croplands and managed peatlands). Although we estimated carbonate contributions with certain limitations (Supplement S7), we were unable to accurately correct the ^{14}C signature of heterotrophically respired CO_2 because the isotopic signatures of endmembers required for this correction (i.e., carbonate, SOC-derived CO_2) could not be sufficiently constrained. Nevertheless, we provide estimated contributions and corrected $\Delta^{14}CO_2$ signatures in Table S2. Our estimations revealed that the mean effect of carbonate weathering on total heterotrophic respiration and on *in situ* soil respiration was < 5±3 % and < 2±1 %, respectively (Table S2).

2.7 Estimation of ages from $\Delta^{14}CO_2$ signatures

We estimated ages of CO_2 from heterotrophic respiration (total, topsoil and subsoil layers) and total soil respiration using carbonate-corrected $\Delta^{14}CO_2$ values with the web-based OxCal software (2024; Bronk Ramsey, 2009) using the Bomb21NH1 calibration curve (Hua et al., 2022). In cases where the $\Delta^{14}CO_2$ values were outside the calibration range (younger than 2019), ages were derived by comparing $\Delta^{14}CO_2$ values with extended bomb curve data. The curve Bomb21NH1 was extended with

$\Delta^{14}CO_2$ values measured at Jungfraujoch, Switzerland by ICOS between 2022 to 2023 (Emmenegger et al., 2024) and in 2024 by Geissbühler et al., in prep.. A detailed description of the approach is presented in Supplement S3.

2.8 Source partitioning using Bayesian mixing models and correction for atmospheric background

The soil respired CO_2 (SR) that we captured *in situ* from the chamber headspace was partitioned into autotrophic (AR) and heterotrophic (HR from each depth layer) sources, as well as residual atmospheric air (ATM) using Bayesian mixing model approaches: MixSIAR (R package MixSIAR, version 3.1.12; Moore & Semmens, 2008; Stock et al., 2018) and an implementation using Python. Partitioning was performed for each site separately. The models use Markov Chain Monte Carlo to sample possible distributions so that:

$$\Delta^{14}CO_{2_{SR}} = f_{ATM}\Delta^{14}CO_{2_{ATM}} + f_{AR}\Delta^{14}CO_{2_{AR}} + \sum_{depth=1}^{n} f_{HR,depth}\Delta^{14}CO_{2_{HR,depth}} \quad (1)$$

$$\delta^{13}CO_{2_{SR}} = f_{ATM}\delta^{13}CO_{2_{ATM}} + f_{AR}\delta^{13}CO_{2_{AR}} + \sum_{depth=1}^{n} f_{HR,depth}\delta^{13}CO_{2_{HR,depth}} \quad (2)$$

$$1 = f_{ATM} + f_{AR} + \sum_{depth=1}^{n} f_{HR,depth} \quad (3)$$

where $0 \leq f \leq 1$ is the proportional contribution of each endmember to total soil respiration and n is the number of incubated depth layers. Input data were $\Delta^{14}CO_2$ values and associated measurement errors (~ 2 ‰) as well as $\delta^{13}CO_2$ values and associated standard deviations of three replicates (~ 0–1 ‰) for mixtures and sources. Constraints and modification of input data are presented in Supplement S4. To estimate the heterotrophic contribution of each depth layer to in situ soil respiration, respiration rates measured at 22 °C were adjusted to field temperature using a uniform Q_{10} of 2.4 (Raich & Schlesinger, 1992), together with depth-related temperature corrections (Bourletsikas et al., 2023). The resulting temperature-adjusted rates were then used as weighting factors in the Bayesian mixing model to improve model performance. In the Bayesian mixing model in Python, we treated heterotrophic respiration from each depth layer as a separate source and added weighted respiration rates as deterministic predictors (assumed uncertainty = 10 %). In MixSIAR, we aggregated depths to topsoil (0-5, 5-10 cm) and subsoil (10-20, 20-40, 40-maximum depth cm) layers to reduce the number of sources in favour of the model performance. Respective isotopic endmember values (topsoil and subsoil) were calculated using a mass balance approach. Isospace plots of MixSIAR are presented in Fig. S10 – Fig. S18. In MixSIAR we used weighted contributions of topsoil and subsoil to total heterotrophic respiration to set up an informative prior with the flat Dirichlet distribution, so that: $\alpha = (f_{ATM}, f_{AR}, \sum f_{HR,depth})$ corresponds to $\alpha = (1, 1, 1)$. Model convergence was assessed via Gelman-Rubin (values < 1.05) and Geweke diagnostics. Further information on model settings is given in Table S1. We combined the mean values and standard deviations of both models to account for specific model restrictions and variability in model outputs. A detailed description of the differences and limitations of the two approaches (MixSIAR and implementation in Python) is given in Supplement S5.

To exclude atmospheric contribution to total soil respiration, we adjusted mean values and standard deviations of autotrophic and heterotrophic contributions so that:

$$f_{AR_{corr}} = \frac{f_{AR}}{1 - f_{ATM}} \quad (4)$$

$$\sum_{depth\,=\,1}^{n} f_{HR,depth_{corr}} = \frac{\sum_{depth\,=\,1}^{n} f_{HR,depth}}{1 - f_{ATM}} \quad (5)$$

We further corrected $\Delta^{14}CO_2$ and $\delta^{13}CO_2$ values of *in situ* soil respiration for the effect of atmospheric background using the proportions of source contributions from the model outputs. We calculated the corrected isotopic values (SR_{corr}) as:

$$\Delta^{14}CO_{2_{SR_{corr}}} = \frac{\Delta^{14}CO_{2_{SR}} - (\Delta^{14}CO_{2_{ATM}} \times (1 - f_{SR}))}{f_{SR}} \quad (6)$$

$$\delta^{13}CO_{2_{SR_{corr}}} = \frac{\delta^{13}CO_{2_{SR}} - (\delta^{13}CO_{2_{ATM}} \times (1 - f_{SR}))}{f_{SR}} \quad (7)$$

where f_{SR} is the fraction of soil-derived CO_2 calculated as the sum of autotrophic and heterotrophic source proportions as initially derived from the model outputs.

3 Results

3.1 *In situ* soil respiration rates across land-use types and seasons

Average *in situ* respiration rates across land-use types ranged from 125 to 363 mg CO_2-C m^{-2} h^{-1} in July/August and from 91 to 191 mg CO_2-C m^{-2} h^{-1} in March (Table 2, Fig. 1). Forests exhibited the lowest respiration rates in both seasons. In July/August, managed peatlands had the highest respiration rates, however, this was mainly related to very high respiration at one of the sites (Lindergut). While the effects of land-use types on *in situ* soil respiration were not significant ($p = 0.133$), seasonality had a significant effect ($p < 0.001$) (Table S4). In agreement with the seasonality, *in situ* respiration rates were affected significantly by soil temperature ($p < 0.001$) and soil water content ($p = 0.002$) (Table S3). While grasslands had soil water contents above 45 vol-%, forest and cropland sites exhibited particularly low soil water contents in July/August (< 20 vol-%; Fig. 1).

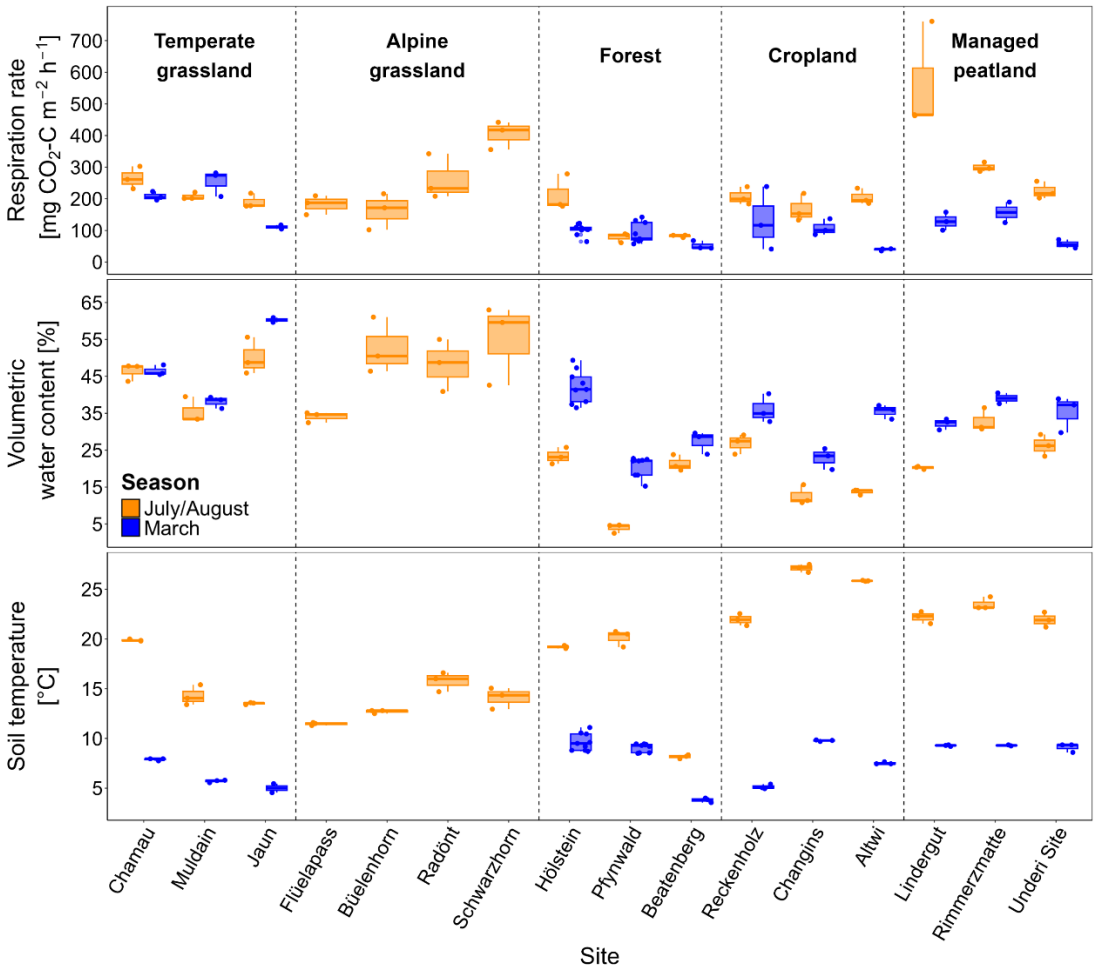

Figure 1: Soil respiration rates (mg CO_2-C m^{-2} h^{-1}), volumetric water content (VWC; vol-%), and soil temperature (°C) from *in situ* measurements in July/August and March across sites and land-use types. Dots indicate replicate measurements boxplots represent summary statistics for each site. VWC and soil temperature are presented for 0-10 cm of the mineral soil (excluding organic layers in forests).

3.2 $\Delta^{14}CO_2$ values in total soil respiration across land-use types and seasons

The soil-respired $\Delta^{14}CO_2$ values measured *in situ* varied significantly across land-use types (p = 0.001 and p = 0.002 with and without managed peatlands (Table S4), with the highest $\Delta^{14}CO_2$ values in forests, followed by grasslands, croplands, and managed peatlands. The latter showed strongly ^{14}C-depleted values (i.e., $\Delta^{14}CO_2$ < -50 ‰; Fig. 2).

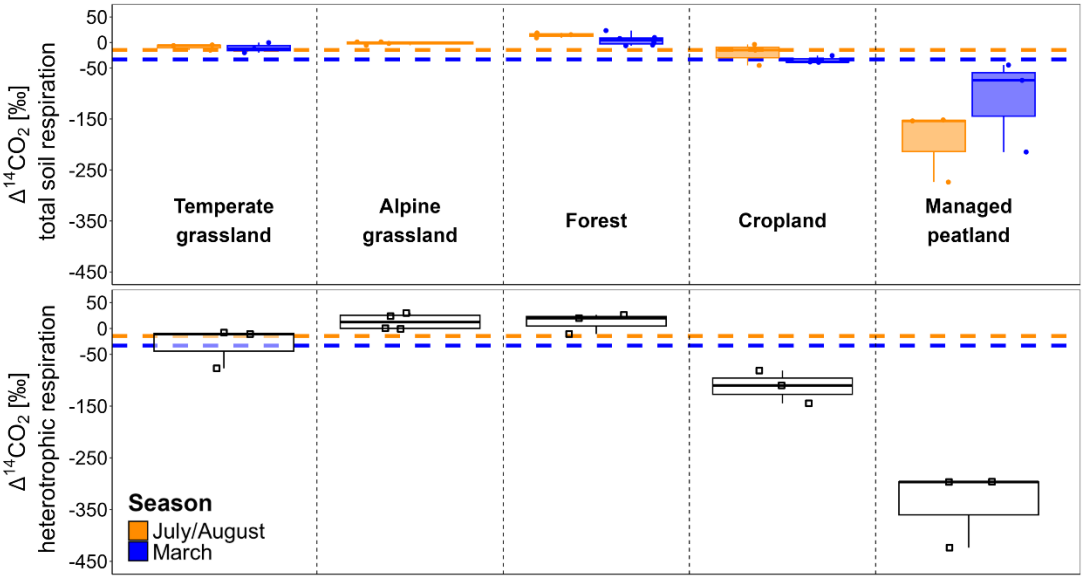

Figure 2: $\Delta^{14}CO_2$ values (‰) of total soil respiration (top) in both seasons and heterotrophic respiration (bottom) across land-use types. Dashed horizontal lines indicate mean atmospheric background $\Delta^{14}CO_2$ levels across land-use types in July/August and March. Note that $\Delta^{14}CO_2$ values of some sites and depths might be influenced by carbonate weathering, which can lower these values. However, the resulting effect on total heterotrophic and total soil respiration is small, and the overall trends remain unchanged (Table S2).

The *in situ* soil-respired $^{14}CO_2$ in croplands and grasslands exhibited modern values, close to the contemporary atmospheric $^{14}CO_2$, corresponding to ages < 10 years (Table 2). Within grasslands, $\Delta^{14}CO_2$ values significantly increased (p = 0.006) with elevation (Fig. S3, Table S5). Forest soils released CO_2 with positive $\Delta^{14}C$ values, indicative of bomb-derived, decadal-old CO_2 (Table 2). In managed peatlands, soil-respired CO_2 had very low $\Delta^{14}CO_2$ values, corresponding to mean ages of approximately 1500 years (Table 2).

The $\Delta^{14}CO_2$ values of total soil respiration differed significantly between July/August and March (p = 0.001) with $\Delta^{14}CO_2$ values being generally closer to atmospheric CO_2 in March. However, the effect of seasonality varied significantly across land-use types (p < 0.001). While managed peatlands exhibited the largest seasonal changes in soil-respired $\Delta^{14}CO_2$, temperate grasslands and forests showed the lowest seasonal variation (Fig. 2, Table 2).

Table 1: Mean soil respiration rates, $\Delta^{14}CO_2$ values, estimated ages and relative source contribution of heterotrophic and autotrophic sources across land-use types. Carbonate-corrected $\Delta^{14}CO_2$ values were used for the estimation of ages (Table S2). Data is reported as means ± standard deviations across sites within land-use types.

	Land-use type									
	Temperate grassland		Alpine grassland		Forest		Cropland		Managed peatland	
Season	July/ August	March	July/ August	March	July/ August	March	July/ August	March	July/ August	March
Total soil respiration										
Respiration rate [mg CO_2-C m^{-2} h^{-1}]	221 ± 39	191 ± 73	253 ± 110	-	125 ± 76	91 ± 29	193 ± 22	93 ± 48	363 ± 178	144 ± 52
$\Delta^{14}CO_2$ value [‰]	-9 ± 6	-11 ± 10	-1 ± 3	-	14 ± 5	5 ± 10	-21 ± 21	-34 ± 7	-193 ± 70	-111 ± 91
Estimated age [yrs]	8 ± 1	7 ± 1	5	-	11 ± 1	9 ± 1	162 ± 12 / 7 ± 1*	230 ± 32 / 5*	1486 ± 47	828 ± 23
Heterotrophic respiration										
Estimated $\Delta^{14}CO_2$ value [‰]										
Total	-32 ± 39		13 ± 16		12 ± 20		-112 ± 32		-339 ± 73	
Organic layer					6 ± 18					
Topsoil	1 ± 13		31 ± 22		23 ± 16		-109 ± 62		-167 ± 27	
Subsoil	-56 ± 58		-41 ± 17		-54 ± 83		-107 ± 50		-349 ± 75	
Estimated age [yrs]										
Total	9 ± 1		40 ± 3		11 ± 1		648 ± 32		3188 ± 46	
Organic layer					7					
Topsoil	7		12 ± 1		11 ± 1		241 ± 16		1394 ± 26	
Subsoil	39		387 ± 14		142 ± 4		729 ± 19		3294 ± 48	
Rel. source contribution [%]										
Total	40 ± 5	46 ± 5	37 ± 5	-	69 ± 7	53 ± 4	31 ± 1	11 ± 2	53 ± 7	23 ± 4
Organic layer					21 ± 4	34 ± 2				
Topsoil	25 ± 4	21 ± 2	29 ± 4	-	44 ± 5	5 ± 0	18 ± 1	3 ± 2	5 ± 5	3 ± 3
Subsoil	15 ± 2	24 ± 4	9 ± 2	-	5 ± 0	16 ± 0	12 ± 1	8 ± 1	48 ± 4	20 ± 2
Autotrophic respiration										
Estimated $\Delta^{14}CO_2$ value [‰]	-12 ± 4	-15 ± 6	-6 ± 3	-	-4 ± 4	-9 ± 5	-13 ± 3	-32 ± 4	-14 ± 4	-34 ± 3
Rel. source contribution [%]	60 ± 7	54 ± 5	63 ± 6	-	31 ± 5	47 ± 3	69 ± 6	89 ± 3	47 ± 6	77 ± 3

** For total soil respiration in croplands, two age ranges are possible. Highly C^{14} depleted atmospheric background samples for these sites make it difficult to interpret the depleted $\Delta^{14}CO_2$ values of total soil respiration. The values are within a range that the comparison with the site-adjusted bomb curves would reveal ages of around 7 and 5 years in July/August and March, respectively. The low relative source proportion of heterotrophic respiration is further indicative of an overall respiration of younger CO_2.*

3.3 Isotopic signatures of atmosphere, autotrophic, and heterotrophic respiration

Our results showed seasonal variation in $\Delta^{14}CO_2$ values of atmosphere and autotrophic respiration (Fig. S4). In the atmosphere, the mean $\Delta^{14}CO_2$ value was more depleted in March than in July/August at all sites (mean across all sites: -14±10 ‰ in July/August and -33±10 ‰ in March), generally related to reduced respiratory activity and seasonal variation in atmospheric transport of CO_2 (Schuur et al., 2016). Due to the proximity of cropland sites to fossil CO_2 sources (i.e., highways, larger roads), their atmospheric $\Delta^{14}CO_2$ values were more depleted than for other land-use types (Fig. S4). Autotrophic $\Delta^{14}CO_2$ signatures were generally close to atmospheric $\Delta^{14}CO_2$ values and followed their seasonal trend with more depleted $\Delta^{14}CO_2$ values in March. In forests, however, autotrophic $\Delta^{14}CO_2$ signatures in March were similar to those in July/August (Fig. S4). Generally, the $\Delta^{14}CO_2$ values from heterotrophic respiration indicate a continuous increase in the age of respired CO_2 with increasing soil depth, which was consistent across all land-use types (Fig. 3). However, $\Delta^{14}CO_2$ values from two cropland sites increased from very depleted values at 0-5 cm to less depleted values at 5-10 cm soil depth.

The variation of $\Delta^{14}CO_2$ values of total heterotrophic respiration across land-use types followed a similar pattern as that of total soil respiration. Temperate grassland soils released the most contemporary CO_2 with ages < 10 years, while alpine grassland and forest soils released bomb-derived, decadal-old CO_2 with average ages of ~ 40 and 11 years, respectively (Table 2). Within grasslands, heterotrophic respiration from topsoil layers exhibited an even stronger increase of $\Delta^{14}CO_2$ values with elevation than *in situ* soil respired CO_2 (p = 0.056; Fig. 3, Fig. S3, Table S5). In contrast, heterotrophic CO_2 in subsoil layers did not show an elevational pattern but showed depleted $\Delta^{14}C$ values for all grassland sites corresponding to ages of 387 years (Fig. 3). Cropland soils released ~ 650-year-old CO_2 and managed peatland even emitted ~ 3200-year-old CO_2 ($p_{land\text{-}use\ type}$ < 0.001; Fig. 2, Table 2, Table S4).

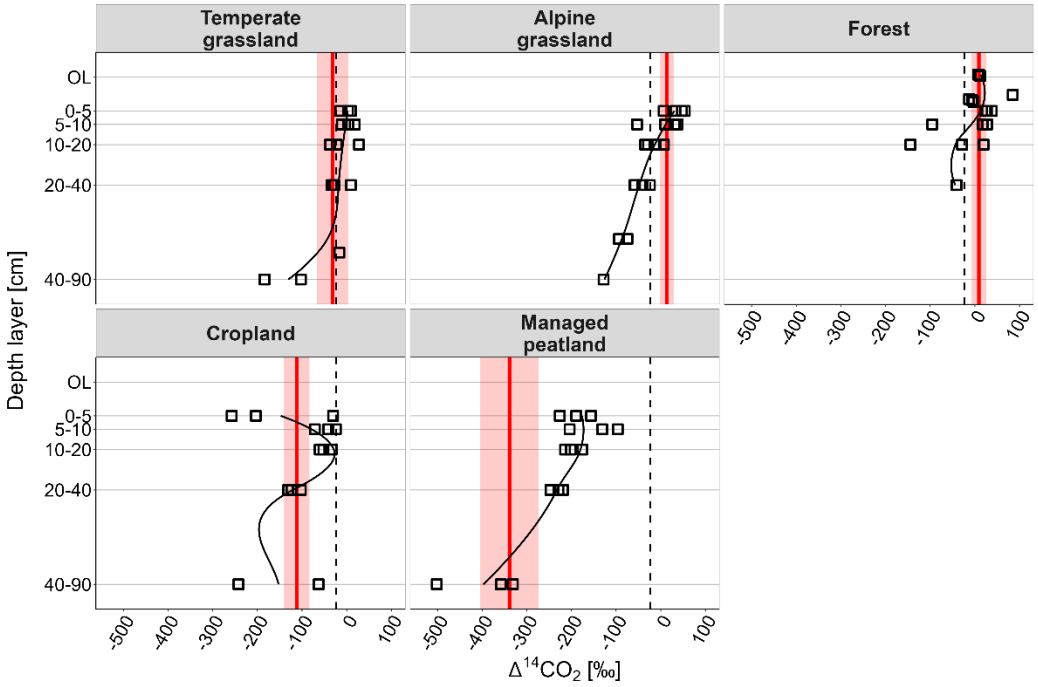

Figure 3: Depth profiles of $\Delta^{14}CO_2$ signatures (‰) of heterotrophic respiration and weighted $\Delta^{14}CO_2$ values of total heterotrophic respiration (red line) and error range (red shaded area). Dashed black vertical lines indicate the mean atmospheric $\Delta^{14}CO_2$ value during our sampling campaigns across all land-use types and both seasons (-24 ‰).

3.4 SOC decomposability

SOC decomposability, measured by the CO_2 release from soils under standardized conditions, varied significantly across land-use types in both topsoil ($p < 0.001$) and subsoil ($p = 0.002$), following a general pattern of decreasing decomposability with increasing soil depth (Fig. 4, Table S4). Croplands and managed peatlands exhibited the lowest values (< 20–60 µg CO_2-C g^{-1} SOC h^{-1}), while forests showed high decomposability in the organic layer (> 200 µg CO_2-C g^{-1} SOC h^{-1}), but much lower levels in the mineral soil. In Pfynwald, SOC decomposability in the organic layer was restricted due to low soil moisture conditions (Figure 1). Temperate grasslands had intermediate decomposability in topsoil and lower values in subsoil. Alpine grasslands exhibited the highest values (46–257 µg CO_2-C g^{-1} SOC h^{-1}), with increased decomposability at higher elevations.

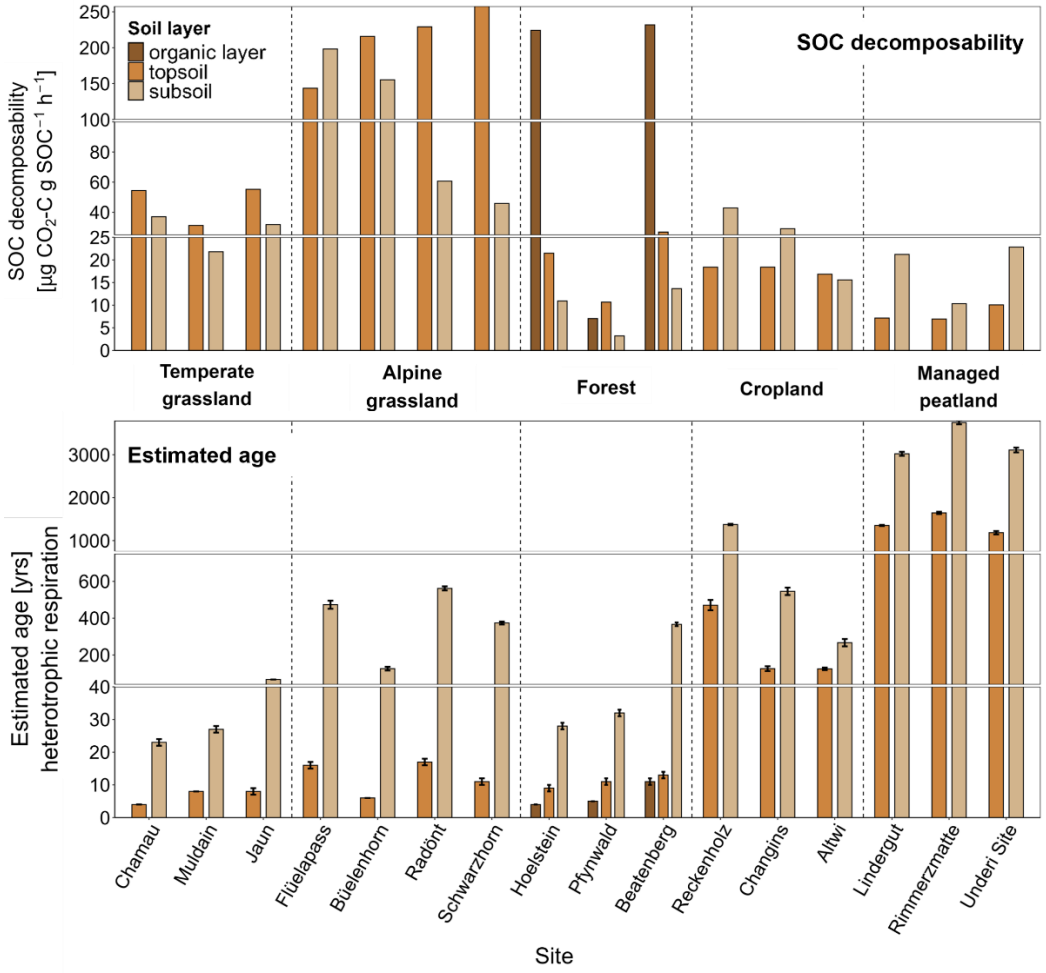

Figure 4: SOC decomposability (top; µg CO_2-C g SOC^{-1} h^{-1}) and estimated ages of heterotrophic respiration (bottom) across land-use types and individual sites for organic layers, topsoil, and subsoil. Error bars for estimated ages represent propagated uncertainties corresponding to the OxCal confidence intervals derived from seasonal estimates. Note that the breaks in the y-axes have different scales for better visualisation.

3.5 Changes in source contribution across land-use types

The $\Delta^{14}CO_2$ signatures of total soil respiration fell between $\Delta^{14}CO_2$ values of autotrophic and heterotrophic endmembers, indicating both contributed to total soil respiration (Fig. S6). Although the difference in source contribution across land-use types was not statistically significant (p = 0.071), distinct patterns existed (Fig. 5, Table S4). Overall, autotrophic respiration was the dominant source of total soil respiration across all land-use types and both seasons (~ 60 %) (Fig. 5, Table 2). The average autotrophic contribution was greatest in croplands (~ 80 %) followed by managed peatlands and grasslands (~ 60 %). Forest showed the smallest average autotrophic contribution (~ 40 %) and accordingly, was the only land-use type where heterotrophic respiration dominated total soil respiration. The relative contribution of heterotrophic respiration was generally higher in July/August than in March for all land-use types except croplands (Fig. 5, Table 2). Managed peatlands showed the

strongest seasonal variation of source contribution with an average heterotrophic contribution of 47 % in July/August and 17 % in March.

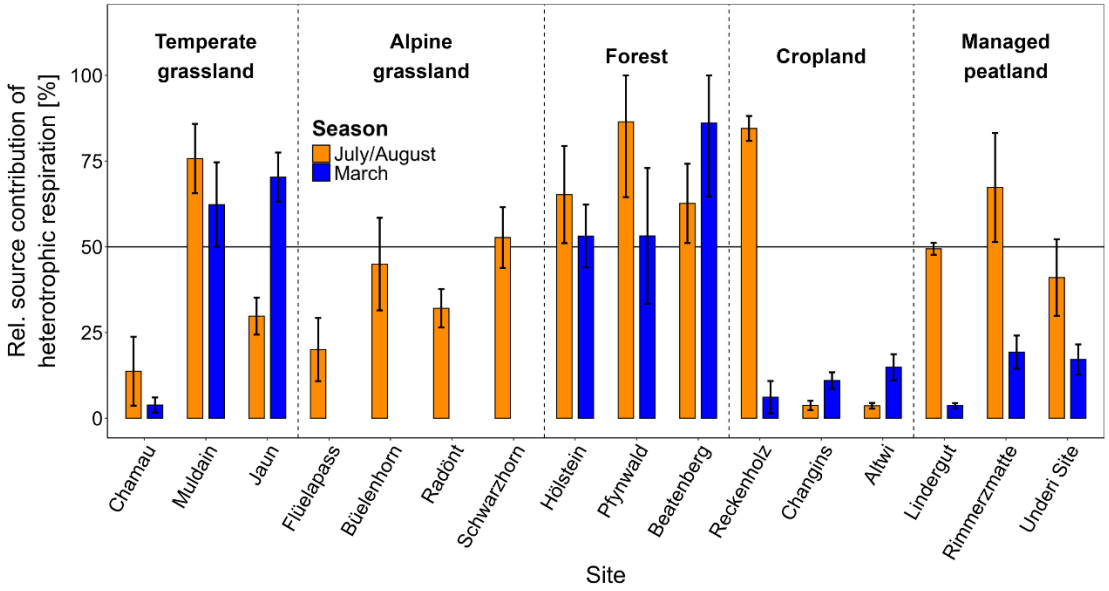

Figure 5: Relative source contribution of heterotrophic respiration in July/August and March across all land-use types and individual sites. Bars represent combined mean values and error bars combined standard deviations from the model outputs.

Measurements of the isotopic composition of heterotrophically respired CO_2 across various depths revealed differences in the contributions of organic layer, topsoil, and subsoil layers to total soil respiration among land-use types. Topsoils were the dominant heterotrophic source in grasslands (~ 26 %) in both seasons and in forests during July/August (44 %) (Table 2, Fig. 3). In forests, the organic layer contributed substantially to total soil respiration in both seasons (21 % in July/August and 34 % in March). In croplands, the generally low contribution of heterotrophic respiration showed similar contributions from top- and subsoil layers (Table 2, Fig. 3). Managed peatlands were almost entirely dominated by heterotrophic respiration from subsoil layers in July/August (48 % of total soil respiration) while subsoil contributions were significantly reduced in March (Table 2).

4 Discussion

Our $\Delta^{14}CO_2$ measurements clearly document that *in situ* soil respiration from all land-use types, except from managed peatlands, was dominated by relatively young C (< 12 years old). In addition, mineralized CO_2 from total heterotrophic respiration showed young C release (< 40 years old) from all land use types, except from managed peatlands and croplands. This pattern indicates that when C enters the soil system, the largest fraction gets rapidly respired back to the atmosphere. Although soil-respired CO_2 was predominantly young, estimated mean ages varied from < 10 years in grasslands to ~ 10 years in forests, and reached up to ~ 1500 years in managed peatlands. In conjunction with variations in soil respiration rates and

SOC decomposability across land-use types, the ^{14}C-derived ages in soil-respired CO_2 provide evidence that the magnitude, velocity, and pathways of C cycling within the plant-soil regime vary among these systems. Although there was variation in environmental conditions (i.e. soil moisture, soil temperature) within individual land-use types across different sites, the overarching patterns distinguishing land-use types remained consistent and site-level variability was accounted for in the statistical analysis. This suggests that land use played a more significant role in shaping respiration dynamics than site-specific environmental conditions.

Here, we propose that SOC decomposability, *in situ* soil respiration rates and ^{14}C-derived ages of soil-respired CO_2 can serve as comprehensive indicators to categorize C cycling into five different systems: (1) high-throughput systems characterized by rapid C cycling – temperate grasslands, (2) temperature-constrained retarding systems characterized by slow C cycling – alpine grasslands, (3) input-constrained retarding systems with a delayed transfer of assimilates back to the atmosphere through soil respiration – forests, (4) C-depleted systems, where reduced C inputs result in the depletion of recent C material and SOC stocks – intensively managed croplands, and (5) hotspots of old soil C release due to significant disturbances in natural C cycling – managed peatlands.

4.1 High-throughput systems – temperate grasslands

Among all land-use types, temperate grasslands represent the land-use type with the highest rates and the youngest age of soil-respired CO_2, characterizing them as high-throughput systems. The high respiration rates in grasslands are consistent with those observed across European land-use types (Schaufler et al., 2010). Here, we show that temperate grasslands have high contributions of autotrophic respiration (60 %), indicating that a large fraction of their high GPP (Schulze et al., 2009) is rapidly allocated to the belowground, where it is metabolized and respired. Among land-use types, grasslands typically show the densest rooting system, the highest root turnover (E. F. Solly et al., 2014), rapid belowground C allocation (Fuchslueger et al., 2016) and a particularly high rhizodeposition (R. Wang et al., 2021). Our study reveals young ages of heterotrophically respired CO_2 and in bulk SOC in topsoil layers (Fig. 3, Fig. S7), indicating that plant-derived C inputs into the soil are rapidly processed by soil microbes. Overall, this results in rapid C cycling through the plant-soil system in temperate grasslands.

4.2 Temperature-constrained retarding systems – alpine grasslands

Our assessment of grassland sites, spanning an elevation gradient from 390 to 2630 m a.s.l., shows increasing ^{14}C-derived ages of soil-respired CO_2 and SOC with elevation (Fig. S3). Since autotrophic respiration dominated irrespective of elevation, the increasing age of in situ soil-respired CO_2 with elevation derives from microbial processing of older SOC at higher elevation. In support, the $\Delta^{14}CO_2$ values of heterotrophic respiration in topsoil layers increased with elevation (Fig. S3), indicating enhanced respiration of bomb-derived, decadal old C. At the same time, Bayesian mixing models showed topsoil layers to contribute more strongly to heterotrophic respiration with increasing elevation. Overall, these findings indicate a slowing of C cycling towards colder climatic conditions in alpine grasslands, reaching MAT's as low as -1.4°C, with shallower and more acidic soils (Table 1). In support, (Leifeld et al., 2009) observed an increasing age in particulate organic matter in grassland

soils especially in deeper soils, which was related to the reduced productivity in alpine grasslands, a shallower rooting depth, and a low microbial activity at low mean annual temperatures. Our finding of the highest SOC decomposability in alpine grasslands among all land-use systems shows that these soils contain the largest amount of readily decomposable SOC (Fig. 4). Along with their high ^{14}C ages in SOC, this suggests that the retarded processing of C inputs into the soil has led to the retention and accumulation of labile C. This, in turn, indicates that alpine grasslands are particularly vulnerable to C cycle perturbations induced by climate warming or by disturbances, potentially leading to losses of old but non-stabilized C.

4.3 Input-constrained retarding systems - forests

In comparison to the other land-use types, forests showed the lowest respiration rates, the greatest contribution of heterotrophic respiration and released the oldest CO_2 via *in situ* soil respiration among undisturbed ecosystems.

The low respiration rates and high relative contributions of heterotrophic respiration is likely the combined effect of a less dense, but deeper rooting system (Jackson et al., 1996), the retarded assimilate transfer to the rhizosphere (Gao et al., 2021) and a larger aboveground C allocation (Schaufler et al., 2010), as well as high heterotrophic contributions from the organic layer (21-34%) to total soil respiration.

Beyond the lower and slower belowground allocation, elevated $\Delta^{14}CO_2$ values of heterotrophic respiration indicate that the release of older CO_2 from forest soils also derives from the decomposition of decadal-old SOC compared with temperate grasslands (Fig. S7). This, in turn, implies slower turnover of plant-derived C in SOC in forests as compared to other land-use types (for croplands and managed peatlands the very old age of heterotrophically respired CO_2 primarily derives from the decomposition of preserved, old C). While slower turnover in alpine grasslands can be associated with colder climatic conditions, higher ages of SOC and respired CO_2 in forests likely derive from both the input of older below- and aboveground C to the soil (E. Solly et al., 2013) and its lower quality slowing decomposition. Forest litter is often enriched in lignin and polyphenols, and nutrient-poorer than grassland litter, and thus more recalcitrant (Zhang et al., 2008). In addition, an acidic soil environment induced by needle litter in coniferous forests together with cold and moist conditions, suppresses microbial and faunal activity (Desie et al., 2020; Zhang et al., 2008), which results in a build-up of thick organic layers (as in Beatenberg) (Hiltbrunner et al., 2013). Our source partitioning revealed that organic layers were major contributors to total heterotrophic respiration (~ 30 % in July/August and ~ 60 % in March). Combined with the substantial contributions of total heterotrophic respiration (53-69 %), this resulted in the highest ^{14}C-derived age of *in situ* soil-respired CO_2 among semi-natural ecosystems. Although climatic differences among forest sites, ranging from hot, dry summer conditions in inner-alpine valleys to cold, wet conditions in subalpine forests, resulted in variations in in situ respiration rates and SOC decomposability, the ages and source contributions of respired CO_2 remained relatively consistent across sites. This suggests that land-use type exerts a stronger control on C cycling pathways than short-term climatic variability, even though the latter affects instantaneous respiration fluxes.

4.4 C-depleted systems – intensively managed croplands

Our results show that while croplands had $\Delta^{14}CO_2$ values in *in situ* soil respiration close to atmospheric $\Delta^{14}CO_2$ values, their heterotrophically respired CO_2 and bulk SOC had pre-bomb ^{14}C levels and were thus depleted in ^{14}C compared to forests and grasslands (Fig. 2, Fig. S7). This overall pattern reveals a high autotrophic contribution in croplands, releasing contemporary C, as well as a long-term depletion of SOC. The latter is likely caused by continuous biomass removal during harvest and the small belowground C input reducing SOC storage (Don et al., 2011; Keel et al., 2019). Losses of SOC can additionally be fostered by soil tillage destroying soil aggregates (e.g., Six et al., 1999), generally leaving SOM with a relatively larger fraction of persistent, old C. In agreement, our study shows that along with the depletion of ^{14}C in soil respired CO_2 and SOC compared to forests and grasslands, cropland soils also showed a low SOC decomposability and the smallest SOC stocks among all land-use types (Fig. 5, Fig. S8). This suggests that these cropland soils are subjected to net C losses, aligning with observations from Swiss long-term experiments that show declining SOC stocks in intensively managed croplands, which had previously been used as grasslands (Keel et al., 2019). The depletion of labile SOC is likely particularly pronounced in the investigated croplands, as they have been continuously managed as croplands for more than 35 years, likely even more than 100 years.

It should be noted that the CO_2 released from two cropland sites (Altwi, Changins) is likely affected by carbonate weathering induced by liming practices, which led to relatively high $^{13}CO_2$ and highly depleted $^{14}CO_2$ values released from the topsoil (Figure 4). However, isotope mixing revealed that potential carbonate weathering contributed < 1 % to total soil respiration in croplands. This is consistent with e.g., (Schindlbacher et al., 2015, 2019; Serrano-Ortiz et al., 2010) who suggest that CO_2 release from carbonates makes a minor contribution to soil-respired CO_2. In addition, potential carbonate contribution did not affect estimates of autotrophic contributions to total soil respiration. ^{14}C-derived ages were estimated using carbonate-corrected ^{14}C values (Supplement S6, Table S2).

Autotrophic contributions in croplands found in this study (July/August: 69 %, March: 89 %) align with previous studies using ^{14}C and ^{13}C labelling approaches (Søe et al., 2004; Werth & Kuzyakov, 2008). Low heterotrophic contributions are likely due to small litter inputs and poor decomposability of the remaining old SOC (Fig. S7). We further assume that high relative autotrophic contributions are also related to hampered heterotrophic respiration due to adverse soil environmental conditions. The two sites, Altwi and Changins, with exceptionally high autotrophic contributions (96 %), exhibited very low water contents (< 15 vol-%). In contrast, the Reckenholz site, with moderate moisture levels (27 vol-%), showed a much lower autotrophic contribution of only 15 % (Fig. 1, Fig. 5). The low water contents in cropland surface soils are probably due to the sparse vegetation cover which enhances evaporative water losses.

4.5 Hotspots of C release – managed peatlands

Despite the dominant contribution of autotrophic respiration to total soil respiration (mean across all managed peatland sites: 68±19 %), managed peatlands released millennial-old CO_2 at a high rate which indicates substantial C losses and advanced degradation in these systems. The release of old, pre-bomb CO_2 has also been observed for other drained and managed

peatlands in Switzerland (Bader et al., 2017; Y. Wang et al., 2021) and can be related to the ~ 150-year long aeration following drainage, which has induced the decomposition of peat material that had previously been protected by anaerobic water-saturated conditions. At our sites, the low SOC decomposability in conjunction with high $\Delta^{14}CO_2$-derived ages (Fig. 5) indicates not only the immediate mobilization of older C following aeration, but also an advanced degradation stage of the peat soil.

The autotrophic contribution (47 % in July/August, 77 % in March) to total soil respiration that we estimated for managed peatlands agrees well with contributions found in natural peatlands during the growing season, where ^{14}C pulse-labelling and trenching approaches revealed autotrophic respiration to contribute between 35 and 61 % (Crow & Wieder, 2005; Wunderlich & Borken, 2012) to total soil respiration. The observed seasonal differences in autotrophic contributions support that water table depth plays a crucial role for the sources of respired CO_2 (Rankin et al., 2023; Stuart et al., 2023). Counterintuitively, the autotrophic contribution to soil respiration was lower in July/August than in March, despite the high plant activity during the growing season. Lower heterotrophic contributions in March (Table 2) are likely because of higher water tables (Paul et al., 2021, 2024). Drier conditions in summer aerate larger portions of the peat, thereby enhancing peat decomposition (Rankin et al., 2023; Stuart et al., 2023). Source partitioning further revealed higher heterotrophic contribution from subsoil layers than from topsoil layers in managed peatlands, which contrasts with observations from all other land-use types (Table 2). Higher subsoil contributions likely result from pronounced increases in SOC stocks with depth (Fig. S8, Fig. 5). Respiratory C losses from deeper peat also contribute to the high *in situ* $^{14}CO_2$-ages of ~ 1500 years released from the managed peatlands in July/August.

4.6 Seasonal dynamics in the age of soil respired CO_2 across land-use types

In March, $\Delta^{14}CO_2$ values were generally closer to atmospheric levels than in July/August which we attribute to higher contributions of autotrophic respiration in March. Higher autotrophic contributions in March than in July/August were unexpected, as heterotrophic respiration typically dominates respiration during winter months due to plant dormancy (Dörr & Münnich, 1986; Schindlbacher et al., 2009; Torn et al., 2009; Wang et al., 2000). We attribute these findings to a combined effect of plant phenology and temperature. Generally, autotrophic respiration is rather driven by plant phenology than by temperature (Atarashi-Andoh et al., 2012) thus we likely captured an active state of the phenology in March for grassland and forest sites. In addition, Marchand et al., 2025 revealed that root activity of deciduous tree species is not constrained by low temperatures. In forests, evergreen vegetation, as well as mosses and graminoids on the forest floor might have additionally contributed to autotrophic respiration. In addition to phenology, the greater autotrophic contribution in March could be related to the up to 9 °C higher air than soil temperatures (Fig. S5). While low soil temperature likely restricted heterotrophic respiration, vegetation was possibly metabolically active at higher air temperatures (Ferrari et al., 2018), which overall resulted in a relatively higher autotrophic respiration compared to microbial activity in cold soils. However, also in crop- and managed peatlands, total soil respiration showed more modern $\Delta^{14}CO_2$ values during March as compared to July/August. In addition, Bayesian models estimated high autotrophic contributions during March. For these vegetation-free arable systems, this may

partly result from the release of recent C during decomposition of residual plant material from the summer growing season, which was not adequately reflected in the incubation experiments.

4.7 Study limitations

The present investigation comprises an extensive suite of C isotopic and supporting data from soils across diverse land-use types and ecoregions of Switzerland. Given the logistical and analytical constraints associated with ^{14}C measurements, we strategically focused on sampling in July/August and March to capture the broadest variability in environmental conditions and plant physiological states. As a consequence, our study provides snapshots rather than continuous records of CO_2 ages, source contributions, and soil respiration rates, resulting in limited spatial and temporal coverage. Despite the inherent limitations, the data reveal clear and robust patterns, offering novel and meaningful insights into C cycling pathways across different land-use types.

To exclude aboveground plant respiration from the *in situ* CO_2 flux, vegetation inside the chamber was clipped 1-2 weeks prior to sampling and directly before if there was plant regrowth. While this approach helped isolate soil-respired CO_2, clipping may have influenced the contribution of autotrophic respiration. Some studies have shown that recent clipping can trigger a short-term increase in rhizosphere respiration (Wunderlich & Borken, 2012), potentially leading to an overestimation of autotrophic contributions. However, given the time allowed between clipping and sampling, we assume that the overall impact on autotrophic respiration in our study was limited. In addition, other studies suggest that such effects are only minor or transient (Bahn et al., 2006; Barneze et al., 2024; Zhou et al., 2007). Two additional sources of soil respiration that may contribute to CO_2 sampled during soil incubations remain challenging to account for: carbonate weathering from natural or artificial (liming) sources, and the decomposition of recent plant assimilates, the latter particularly affecting crop- and managed peatlands. In these land-use types, model estimations of high autotrophic contributions during winter might be biased by the release of recent CO_2 from decomposing plant residues from the last growing season, carrying a similar modern $\Delta^{14}C$ than autotrophic respiration. Despite these limitations, clear patterns have emerged from the suite of measurements undertaken as part of this study, providing the basis for a proposed conceptual framework for land-use system categorization based on the rates and ^{14}C signatures of soil respiration.

5 Conclusions

Our study demonstrates that combining measurements of respiration rates and ^{14}C signatures of soil-respired CO_2 – both *in situ* and under controlled incubations – provides valuable insights into C cycling pathways across contrasting land-use types. This combined approach reveals how differences in C inputs, microbial processing, ecosystem-specific constraints, and management practices jointly shape the respiration rate, age, and sources of released CO_2 – ranging from rapid, input-driven cycling of young C with high autotrophic contributions in temperate grasslands to the loss of ancient, previously preserved C via heterotrophic respiration through drainage in managed peatlands. The ^{14}C-based respiration measurements provide a

general framework for identifying systems in which soils retain SOC versus conditions that promote the decomposition and mobilization of older SOC. Applying this approach across broader climatic gradients, soil types, or management regimes could help define transferable indicators of soil C cycling. The integration of rate- and ^{14}C-based measurements of soil respiration may enable more accurate predictions of how soils will respond to future environmental changes.

Code and data availability

The data supporting this study, together with the codes used for the Bayesian mixing model, are publicly available in the open-access Zenodo repository under DOI: https://doi.org/10.5281/zenodo.18067939.

Author Contribution

L. I. M.: conceptualisation, data curation, formal analysis, investigation, methodology, project administration, visualisation, writing – original draft preparation, writing – review and editing. **D. G.:** methodology, writing – review and editing. **S. T.:** investigation, formal analysis. **A. U.:** investigation, methodology, writing – review and editing. **A. S. B.:** methodology, formal analysis, writing – review and editing. **M. M. D.:** investigation, writing – review and editing. **C. M.:** investigation, writing – review and editing. **L. W.:** methodology, resources, writing – review and editing. **P. G.:** methodology, resources. **N. H.:** methodology, resources. **M. E.:** investigation, writing – review and editing. **A. K.:** investigation. **J. L.:** investigation, writing – review and editing. **T. I. E.:** funding acquisition, resources, supervision, writing – review and editing. **F. H.:** conceptualisation, funding acquisition, resources, supervision, writing – original draft preparation, writing – review and editing.

Competing interest

At least one of the (co-)authors is a member of the editorial board of Biogeosciences.

Acknowledgements

We thank Michael Leonardo di Gallo, Logan James Banner, Andrin Bieri, Nik Wirz, Clara Juliette Gund, David Schweizer, Thomas Laemmel, Niek Abram ten Cate, and Dennis Christopher Handte for their support during field work. We further thank Alois Zürcher, Daniel Christen, Daniel Wasner, David Schweizer, Jonathan Frei, Roger Köchli, and Marco Walser for their assistance with the laboratory work. Further thanks to André Albrecht and Urs Ramsperger for their support during sample preparation and measurements of ^{14}C contents and to Alessandro Schlumpf and Ursula Graf for their support during sample preparation and measurements of ^{13}C contents. Special thanks to our colleagues Richard Peters, Thomas Guillaume, Juliane Hirte, Raphaël Wittwer, Sonja Paul Marit, Matthias Volk, Yi Wang, and Nina Buchmann for providing information and access

to sampling sites. We further thank Mirko Städler, René Haselbacher, Peter Röthlisberger, and Matthias Gyger for providing their fields for our sampling. In addition, we thank Claudia Guidi and Katrin Meusburger for their support and scientific input during data analysis.

Financial support

Financial support was provided by the Radiocarbon Inventories of Switzerland project 193770 funded by the Swiss National Science Foundation.

References

Atarashi-Andoh, M., Koarashi, J., Ishizuka, S., & Hirai, K. (2012). Seasonal patterns and control factors of CO2 effluxes from surface litter, soil organic carbon, and root-derived carbon estimated using radiocarbon signatures. *Agricultural and Forest Meteorology*, *152*, 149–158. https://doi.org/10.1016/j.agrformet.2011.09.015

Bader, C., Müller, M., Schulin, R., & Leifeld, J. (2017). Amount and stability of recent and aged plant residues in degrading peatland soils. *Soil Biology and Biochemistry*, *109*, 167–175. https://doi.org/10.1016/j.soilbio.2017.01.029

Bahn, M., Knapp, M., Garajova, Z., Pfahringer, N., & Cernusca, A. (2006). Root respiration in temperate mountain grasslands differing in land use. *Global Change Biology*, *12*(6), 995–1006. https://doi.org/10.1111/j.1365-2486.2006.01144.x

Barneze, A. S., Whitaker, J., McNamara, N. P., & Ostle, N. J. (2024). Interactive effects of climate warming and management on grassland soil respiration partitioning. *European Journal of Soil Science*, *75*(3), e13491. https://doi.org/10.1111/ejss.13491

Bolin, B., & Rodhe, H. (1973). A note on the concepts of age distribution and transit time in natural reservoirs. *Tellus*, *25*(1), 58–62. https://doi.org/10.1111/j.2153-3490.1973.tb01594.x

Borken, W., Savage, K., Davidson, E. A., & Trumbore, S. E. (2006). Effects of experimental drought on soil respiration and radiocarbon efflux from a temperate forest soil. *Global Change Biology*, *12*(2), 177–193. https://doi.org/10.1111/j.1365-2486.2005.001058.x

Bronk Ramsey, C. (2009). Bayesian Analysis of Radiocarbon Dates. *Radiocarbon*, *51*(1), 337–360. https://doi.org/10.1017/S0033822200033865

Butterbach-Bahl, K., Kiese, R., & Liu, C. (2011). Measurements of Biosphere–Atmosphere Exchange of CH4 in Terrestrial Ecosystems. In *Methods in Enzymology* (Vol. 495, pp. 271–287). Elsevier. https://doi.org/10.1016/B978-0-12-386905-0.00018-8

Crow, S. E., & Wieder, R. K. (2005). SOURCES OF CO_2 EMISSION FROM A NORTHERN PEATLAND: ROOT RESPIRATION, EXUDATION, AND DECOMPOSITION. *Ecology*, *86*(7), 1825–1834. https://doi.org/10.1890/04-1575

Desie, E., Van Meerbeek, K., De Wandeler, H., Bruelheide, H., Domisch, T., Jaroszewicz, B., Joly, F., Vancampenhout, K., Vesterdal, L., & Muys, B. (2020). Positive feedback loop between earthworms, humus form and soil pH reinforces earthworm abundance in European forests. *Functional Ecology*, *34*(12), 2598–2610. https://doi.org/10.1111/1365-2435.13668

Diao, H., Wang, A., Yuan, F., Guan, D., & Wu, J. (2022). Autotrophic respiration modulates the carbon isotope composition of soil respiration in a mixed forest. *Science of The Total Environment*, *807*, 150834. https://doi.org/10.1016/j.scitotenv.2021.150834

Don, A., Schumacher, J., & Freibauer, A. (2011). Impact of tropical land-use change on soil organic carbon stocks - a meta-analysis: SOIL ORGANIC CARBON AND LAND-USE CHANGE. *Global Change Biology*, *17*(4), 1658–1670. https://doi.org/10.1111/j.1365-2486.2010.02336.x

Dörr, H., & Münnich, K. O. (1986). Annual Variations of the ^{14}C Content of Soil CO_2. *Radiocarbon*, *28*(2A), 338–345. https://doi.org/10.1017/S0033822200007438

Emmenegger, L., Leuenberger, M., & Steinbacher, M. (2024). *ICOS ATC 14C Release analysed by ICOS CRL, Jungfraujoch (6.0 m), 2015-09-21–2023-10-02* [Data set]. ICOS RI. https://hdl.handle.net/11676/6c_RZ7NHc2dnZv7d84BMY_YY

Eriksson, E. (1971). Compartment Models and Reservoir Theory. *Annual Review of Ecology and Systematics*, *2*(1), 67–84. https://doi.org/10.1146/annurev.es.02.110171.000435

Ferrari, A., Hagedorn, F., & Niklaus, P. A. (2018). Disentangling effects of air and soil temperature on C allocation in cold environments: A^{14} C pulse-labelling study with two plant species. *Ecology and Evolution*, *8*(16), 7778–7789. https://doi.org/10.1002/ece3.4215

Flisch, R., Sinaj, S., Charles, R., & Richner, W. (2009). GRUDAF 2009. Grundlagen für die Düngung im Acker- und Futterbau. In *AGRARForschung* (Vol. 2). Forschungsanstalten Agroscope Changins-Wädenswil ACW und Agroscope Reckenholz-Tänikon ART.

Fuchslueger, L., Bahn, M., Hasibeder, R., Kienzl, S., Fritz, K., Schmitt, M., Watzka, M., & Richter, A. (2016). Drought history affects grassland plant and microbial carbon turnover during and after a subsequent drought event. *Journal of Ecology*, *104*(5), 1453–1465. https://doi.org/10.1111/1365-2745.12593

Gao, D., Joseph, J., Werner, R. A., Brunner, I., Zürcher, A., Hug, C., Wang, A., Zhao, C., Bai, E., Meusburger, K., Gessler, A., & Hagedorn, F. (2021). Drought alters the carbon footprint of trees in soils—Tracking the spatio-temporal fate of^{13} C-labelled assimilates in the soil of an old-growth pine forest. *Global Change Biology*, *27*(11), 2491–2506. https://doi.org/10.1111/gcb.15557

Gautschi, P. (2017). *A new method to graphitize CO2 from atmospheric air for radiocarbon analysis* [Master thesis]. ETH Zurich.

Geissbühler, D., Laemmel, T., Henne, T., Brunner, D., Gautschi, P., Wacker, L., & Szidat, S. (in prep.). *Source apportionment of atmospheric CO2 in air masses transported over Switzerland in a two-year monitoring campaign*.

Graven, H. D., Warren, H., Gibbs, H. K., Khatiwala, S., Koven, C., Lester, J., Levin, I., Spawn-Lee, S. A., & Wieder, W. (2024). Bomb radiocarbon evidence for strong global carbon uptake and turnover in terrestrial vegetation. *Science*, *384*(6702), 1335–1339. https://doi.org/10.1126/science.adl4443

Hagedorn, F., & Joos, O. (2014). Experimental summer drought reduces soil CO2 effluxes and DOC leaching in Swiss grassland soils along an elevational gradient. *Biogeochemistry*, *117*(2–3), 395–412. https://doi.org/10.1007/s10533-013-9881-x

Hanson, P. J., Edwards, N. T., Garten, C. T., & Andrews, J. A. (2000). Separating root and soil microbial contributions to soil respiration: A review of methods and observations. *Biogeochemistry*, *48*, 115–146. https://doi.org/10.1023/A:1006244819642

Hicks Pries, C. E., Schuur, E. A. G., & Crummer, K. G. (2013). Thawing permafrost increases old soil and autotrophic respiration in tundra: Partitioning ecosystem respiration using δ^{13}C and Δ^{14}C. *Global Change Biology*, *19*(2), 649–661. https://doi.org/10.1111/gcb.12058

Hiltbrunner, D., Zimmermann, S., & Hagedorn, F. (2013). Afforestation with Norway spruce on a subalpine pasture alters carbon dynamics but only moderately affects soil carbon storage. *Biogeochemistry*, *115*(1–3), 251–266. https://doi.org/10.1007/s10533-013-9832-6

Hirte, J., Richner, W., Orth, B., Liebisch, F., & Flisch, R. (2021). Yield response to soil test phosphorus in Switzerland: Pedoclimatic drivers of critical concentrations for optimal crop yields using multilevel modelling. *Science of The Total Environment*, *755*, 143453. https://doi.org/10.1016/j.scitotenv.2020.143453

Hua, Q., Turnbull, J. C., Santos, G. M., Rakowski, A. Z., Ancapichún, S., De Pol-Holz, R., Hammer, S., Lehman, S. J., Levin, I., Miller, J. B., Palmer, J. G., & Turney, C. S. M. (2022). ATMOSPHERIC RADIOCARBON FOR THE PERIOD 1950–2019. *Radiocarbon*, *64*(4), 723–745. https://doi.org/10.1017/RDC.2021.95

Intergovernmental Panel On Climate Change (Ipcc). (2021). *Climate Change 2021 – The Physical Science Basis: Working Group I Contribution to the Sixth Assessment Report of the Intergovernmental Panel on Climate Change* (1st edn). Cambridge University Press. https://doi.org/10.1017/9781009157896

IPCC (with IPPC National Greenhouse Gas Inventories Programme). (2003). *Good practice guidance for land use, land-use change and forestry /The Intergovernmental Panel on Climate Change. Ed. By Jim Penman* (J. Penman, Ed.).

Jackson, R. B., Canadell, J., Ehleringer, J. R., Mooney, H. A., Sala, O. E., & Schulze, E. D. (1996). A global analysis of root distributions for terrestrial biomes. *Oecologia*, *108*(3), 389–411. https://doi.org/10.1007/BF00333714

Keel, S. G., Anken, T., Büchi, L., Chervet, A., Fliessbach, A., Flisch, R., Huguenin-Elie, O., Mäder, P., Mayer, J., Sinaj, S., Sturny, W., Wüst-Galley, C., Zihlmann, U., & Leifeld, J. (2019). Loss of soil organic carbon in Swiss long-term

agricultural experiments over a wide range of management practices. *Agriculture, Ecosystems & Environment*, *286*, 106654. https://doi.org/10.1016/j.agee.2019.106654

Komada, T., Anderson, M. R., & Dorfmeier, C. L. (2008). Carbonate removal from coastal sediments for the determination of organic carbon and its isotopic signatures, δ^{13}C and Δ^{14}C: Comparison of fumigation and direct acidification by hydrochloric acid. *Limnology and Oceanography: Methods*, *6*(6), 254–262. https://doi.org/10.4319/lom.2008.6.254

Konings, A. G., Bloom, A. A., Liu, J., Parazoo, N. C., Schimel, D. S., & Bowman, K. W. (2019). Global satellite-driven estimates of heterotrophic respiration. *Biogeosciences*, *16*(11), 2269–2284. https://doi.org/10.5194/bg-16-2269-2019

Kuzyakov, Y. (2006). Sources of CO2 efflux from soil and review of partitioning methods. *Soil Biology and Biochemistry*, *38*(3), 425–448. https://doi.org/10.1016/j.soilbio.2005.08.020

Leifeld, J., Bassin, S., & Fuhrer, J. (2005). Carbon stocks in Swiss agricultural soils predicted by land-use, soil characteristics, and altitude. *Agriculture, Ecosystems & Environment*, *105*(1–2), 255–266. https://doi.org/10.1016/j.agee.2004.03.006

Leifeld, J., Meyer, S., Budge, K., Sebastia, M. T., Zimmermann, M., & Fuhrer, J. (2015). Turnover of Grassland Roots in Mountain Ecosystems Revealed by Their Radiocarbon Signature: Role of Temperature and Management. *PLOS ONE*, *10*(3), e0119184. https://doi.org/10.1371/journal.pone.0119184

Leifeld, J., Müller, M., & Fuhrer, J. (2011). Peatland subsidence and carbon loss from drained temperate fens. *Soil Use and Management*, *27*(2), 170–176. https://doi.org/10.1111/j.1475-2743.2011.00327.x

Leifeld, J., Zimmermann, M., Fuhrer, J., & Conen, F. (2009). Storage and turnover of carbon in grassland soils along an elevation gradient in the Swiss Alps. *Global Change Biology*, *15*(3), 668–679. https://doi.org/10.1111/j.1365-2486.2008.01782.x

Li, W., Ciais, P., Wang, Y., Peng, S., Broquet, G., Ballantyne, A. P., Canadell, J. G., Cooper, L., Friedlingstein, P., Le Quéré, C., Myneni, R. B., Peters, G. P., Piao, S., & Pongratz, J. (2016). Reducing uncertainties in decadal variability of the global carbon budget with multiple datasets. *Proceedings of the National Academy of Sciences*, *113*(46), 13104–13108. https://doi.org/10.1073/pnas.1603956113

Maltas, A., Kebli, H., Oberholzer, H. R., Weisskopf, P., & Sinaj, S. (2018). The effects of organic and mineral fertilizers on carbon sequestration, soil properties, and crop yields from a long-term field experiment under a Swiss conventional farming system. *Land Degradation & Development*, *29*(4), 926–938. https://doi.org/10.1002/ldr.2913

Mann, W. B. (1983). An International Reference Material for Radiocarbon Dating. *Radiocarbon*, *25*(2), 519–527. https://doi.org/10.1017/S0033822200005816

Marchand, L. J., Gričar, J., Zuccarini, P., Dox, I., Mariën, B., Verlinden, M., Heinecke, T., Prislan, P., Marie, G., Lange, H., Van Den Bulcke, J., Penuelas, J., Fonti, P., & Campioli, M. (2025). No winter halt in below-ground wood growth of four angiosperm deciduous tree species. *Nature Ecology & Evolution*. https://doi.org/10.1038/s41559-024-02602-6

Midwood, A. J., Gebbing, T., Wendler, R., Sommerkorn, M., Hunt, J. E., & Millard, P. (2006). Collection and storage of CO_2 for ^{13}C analysis: An application to separate soil CO_2 efflux into root- and soil-derived components. *Rapid Communications in Mass Spectrometry*, *20*(22), 3379–3384. https://doi.org/10.1002/rcm.2749

Millard, P., Midwood, A. J., Hunt, J. E., Barbour, M. M., & Whitehead, D. (2010). Quantifying the contribution of soil organic matter turnover to forest soil respiration, using natural abundance δ13C. *Soil Biology and Biochemistry*, *42*(6), 935–943. https://doi.org/10.1016/j.soilbio.2010.02.010

Moore, J. W., & Semmens, B. X. (2008). Incorporating uncertainty and prior information into stable isotope mixing models. *Ecology Letters*, *11*(5), 470–480. https://doi.org/10.1111/j.1461-0248.2008.01163.x

Nissan, A., Alcolombri, U., Peleg, N., Galili, N., Jimenez-Martinez, J., Molnar, P., & Holzner, M. (2023). Global warming accelerates soil heterotrophic respiration. *Nature Communications*, *14*(1), 3452. https://doi.org/10.1038/s41467-023-38981-w

Oberholzer, H. R., Leifeld, J., & Mayer, J. (2014). Changes in soil carbon and crop yield over 60 years in the Zurich Organic Fertilization Experiment, following land-use change from grassland to cropland. *Journal of Plant Nutrition and Soil Science*, *177*(5), 696–704. https://doi.org/10.1002/jpln.201300385

Oertel, C., Matschullat, J., Zurba, K., Zimmermann, F., & Erasmi, S. (2016). Greenhouse gas emissions from soils—A review. *Geochemistry*, *76*(3), 327–352. https://doi.org/10.1016/j.chemer.2016.04.002

Paul, S., Ammann, C., Alewell, C., & Leifeld, J. (2021). Carbon budget response of an agriculturally used fen to different soil moisture conditions. *Agricultural and Forest Meteorology*, *300*, 108319. https://doi.org/10.1016/j.agrformet.2021.108319

Paul, S., Ammann, C., Wang, Y., Alewell, C., & Leifeld, J. (2024). Can mineral soil coverage be a suitable option to mitigate greenhouse gas emissions from agriculturally managed peatlands? *Agriculture, Ecosystems & Environment*, *375*, 109197. https://doi.org/10.1016/j.agee.2024.109197

Phillips, C. L., McFarlane, K. J., Risk, D., & Desai, A. R. (2013). Biological and physical influences on soil $^{14}CO_2$ seasonal dynamics in a temperate hardwood forest. *Biogeosciences*, *10*(12), 7999–8012. https://doi.org/10.5194/bg-10-7999-2013

Ramsperger, U., De Maria, D., Gautschi, P., Maxeiner, S., Müller, A. M., Synal, H.-A., & Wacker, L. (2024). LEA—A NOVEL LOW ENERGY ACCELERATOR FOR^{14} C DATING. *Radiocarbon*, *66*(5), 1280–1288. https://doi.org/10.1017/RDC.2023.85

Rankin, T., Roulet, N., Humphreys, E., Peichl, M., & Järveoja, J. (2023). Partitioning autotrophic and heterotrophic respiration in an ombrotrophic bog. *Frontiers in Earth Science*, *11*, 1263418. https://doi.org/10.3389/feart.2023.1263418

Rong, Y., Ma, L., Johnson, D. A., & Yuan, F. (2015). Soil respiration patterns for four major land-use types of the agro-pastoral region of northern China. *Agriculture, Ecosystems & Environment*, *213*, 142–150. https://doi.org/10.1016/j.agee.2015.08.002

Ruff, M., Fahrni, S., Gäggeler, H. W., Hajdas, I., Suter, M., Synal, H.-A., Szidat, S., & Wacker, L. (2010). On-line Radiocarbon Measurements of Small Samples Using Elemental Analyzer and MICADAS Gas Ion Source. *Radiocarbon*, *52*(4), 1645–1656. https://doi.org/10.1017/S003382220005637X

Schädel, C., Beem-Miller, J., Aziz Rad, M., Crow, S. E., Hicks Pries, C., Ernakovich, J., Hoyt, A. M., Plante, A., Stoner, S., Treat, C. C., & Sierra, C. A. (2019). *Decomposability of soil organic matter over time: The Soil Incubation Database (SIDb, version 1.0) and guidance for incubation procedures*. Copernicus GmbH. https://doi.org/10.5194/essd-2019-184

Schaufler, G., Kitzler, B., Schindlbacher, A., Skiba, U., Sutton, M. A., & Zechmeister-Boltenstern, S. (2010). Greenhouse gas emissions from European soils under different land use: Effects of soil moisture and temperature. *European Journal of Soil Science*, *61*(5), 683–696. https://doi.org/10.1111/j.1365-2389.2010.01277.x

Schindlbacher, A., Beck, K., Holzheu, S., & Borken, W. (2019). Inorganic Carbon Leaching From a Warmed and Irrigated Carbonate Forest Soil. *Frontiers in Forests and Global Change*, *2*, 40. https://doi.org/10.3389/ffgc.2019.00040

Schindlbacher, A., Borken, W., Djukic, I., Brandstätter, C., Spötl, C., & Wanek, W. (2015). Contribution of carbonate weathering to the CO2 efflux from temperate forest soils. *Biogeochemistry*, *124*(1–3), 273–290. https://doi.org/10.1007/s10533-015-0097-0

Schindlbacher, A., Zechmeister-Boltenstern, S., & Jandl, R. (2009). Carbon losses due to soil warming: Do autotrophic and heterotrophic soil respiration respond equally? *Global Change Biology*, *15*(4), 901–913. https://doi.org/10.1111/j.1365-2486.2008.01757.x

Schulze, E. D., Luyssaert, S., Ciais, P., Freibauer, A., Janssens, I. A., Soussana, J. F., Smith, P., Grace, J., Levin, I., Thiruchittampalam, B., Heimann, M., Dolman, A. J., Valentini, R., Bousquet, P., Peylin, P., Peters, W., Rödenbeck, C., Etiope, G., Vuichard, N., … the CarboEurope Team. (2009). Importance of methane and nitrous oxide for Europe's terrestrial greenhouse-gas balance. *Nature Geoscience*, *2*(12), 842–850. https://doi.org/10.1038/ngeo686

Schuur, E. A. G., Druffel, E., & Trumbore, S. E. (Eds). (2016). *Radiocarbon and Climate Change*. Springer International Publishing. https://doi.org/10.1007/978-3-319-25643-6

Schuur, E. A. G., & Trumbore, S. E. (2006). Partitioning sources of soil respiration in boreal black spruce forest using radiocarbon. *Global Change Biology*, *12*(2), 165–176. https://doi.org/10.1111/j.1365-2486.2005.01066.x

Serrano-Ortiz, P., Roland, M., Sanchez-Moral, S., Janssens, I. A., Domingo, F., Goddéris, Y., & Kowalski, A. S. (2010). Hidden, abiotic CO2 flows and gaseous reservoirs in the terrestrial carbon cycle: Review and perspectives. *Agricultural and Forest Meteorology*, *150*(3), 321–329. https://doi.org/10.1016/j.agrformet.2010.01.002

Shi, B., Fu, X., Smith, M. D., Chen, A., Knapp, A. K., Wang, C., Xu, W., Zhang, R., Gao, W., & Sun, W. (2022). Autotrophic respiration is more sensitive to nitrogen addition and grazing than heterotrophic respiration in a meadow steppe. *CATENA*, *213*, 106207. https://doi.org/10.1016/j.catena.2022.106207

Sierra, C. A., Müller, M., Metzler, H., Manzoni, S., & Trumbore, S. E. (2017). The muddle of ages, turnover, transit, and residence times in the carbon cycle. *Global Change Biology*, *23*(5), 1763–1773. https://doi.org/10.1111/gcb.13556

Six, J., Elliott, E. T., & Paustian, K. (1999). Aggregate and Soil Organic Matter Dynamics under Conventional and No-Tillage Systems. *Soil Science Society of America Journal*, *63*(5), 1350–1358. https://doi.org/10.2136/sssaj1999.6351350x

Søe, A. R. B., Giesemann, A., Anderson, T.-H., Weigel, H.-J., & Buchmann, N. (2004). Soil respiration under elevated CO_2 and its partitioning into recently assimilated and older carbon sources. *Plant and Soil*, *262*(1/2), 85–94. https://doi.org/10.1023/B:PLSO.0000037025.78016.9b

Solly, E. F., Schöning, I., Boch, S., Kandeler, E., Marhan, S., Michalzik, B., Müller, J., Zscheischler, J., Trumbore, S. E., & Schrumpf, M. (2014). Factors controlling decomposition rates of fine root litter in temperate forests and grasslands. *Plant and Soil*, *382*(1–2), 203–218. https://doi.org/10.1007/s11104-014-2151-4

Solly, E., Schöning, I., Boch, S., Müller, J., Socher, S. A., Trumbore, S. E., & Schrumpf, M. (2013). Mean age of carbon in fine roots from temperate forests and grasslands with different management. *Biogeosciences*, *10*(7), 4833–4843. https://doi.org/10.5194/bg-10-4833-2013

Stock, B. C., Jackson, A. L., Ward, E. J., Parnell, A. C., Phillips, D. L., & Semmens, B. X. (2018). Analyzing mixing systems using a new generation of Bayesian tracer mixing models. *PeerJ*, *6*, e5096. https://doi.org/10.7717/peerj.5096

Stuart, J. E. M., Tucker, C. L., Lilleskov, E. A., Kolka, R. K., Chimner, R. A., Heckman, K. A., & Kane, E. S. (2023). Evidence for older carbon loss with lowered water tables and changing plant functional groups in peatlands. *Global Change Biology*, *29*(3), 780–793. https://doi.org/10.1111/gcb.16508

Synal, H.-A., Stocker, M., & Suter, M. (2007). MICADAS: A new compact radiocarbon AMS system. *Nuclear Instruments and Methods in Physics Research Section B: Beam Interactions with Materials and Atoms*, *259*(1), 7–13. https://doi.org/10.1016/j.nimb.2007.01.138

Tangarife-Escobar, A., Guggenberger, G., Feng, X., Muñoz, E., Chanca, I., Peichl, M., Smith, P., & Sierra, C. A. (2024). Radiocarbon Isotopic Disequilibrium Shows Little Incorporation of New Carbon in Mineral Soils of a Boreal Forest Ecosystem. *Journal of Geophysical Research: Biogeosciences*, *129*(9), e2024JG008191. https://doi.org/10.1029/2024JG008191

Tharammal, T., Bala, G., Devaraju, N., & Nemani, R. (2019). A review of the major drivers of the terrestrial carbon uptake: Model-based assessments, consensus, and uncertainties. *Environmental Research Letters*, *14*(9), 093005. https://doi.org/10.1088/1748-9326/ab3012

Torn, M. S., Swanston, C. W., Castanha, C., & Trumbore, S. E. (2009). Storage and Turnover of Organic Matter in Soil. In N. Senesi, B. Xing, & P. M. Huang (Eds), *Biophysico-Chemical Processes Involving Natural Nonliving Organic Matter in Environmental Systems* (1st edn, pp. 219–272). Wiley. https://doi.org/10.1002/9780470494950.ch6

Trumbore, S. (2006). Carbon respired by terrestrial ecosystems – recent progress and challenges. *Global Change Biology*, *12*(2), 141–153. https://doi.org/10.1111/j.1365-2486.2006.01067.x

Wacker, L., Christl, M., & Synal, H.-A. (2010). Bats: A new tool for AMS data reduction. *Nuclear Instruments and Methods in Physics Research Section B: Beam Interactions with Materials and Atoms*, *268*(7–8), 976–979. https://doi.org/10.1016/j.nimb.2009.10.078

Wacker, L., Němec, M., & Bourquin, J. (2010). A revolutionary graphitisation system: Fully automated, compact and simple. *Nuclear Instruments and Methods in Physics Research Section B: Beam Interactions with Materials and Atoms*, *268*(7–8), 931–934. https://doi.org/10.1016/j.nimb.2009.10.067

Walthert, L., Graf, U., Kammer, A., Luster, J., Pezzotta, D., Zimmermann, S., & Hagedorn, F. (2010). Determination of organic and inorganic carbon, δ^{13} C, and nitrogen in soils containing carbonates after acid fumigation with HCl. *Journal of Plant Nutrition and Soil Science*, *173*(2), 207–216. https://doi.org/10.1002/jpln.200900158

Walthert, L., Lüscher, P., Luster, J., & Peter, B. (2002). *Langfristige Waldökosystem-Forschung LWF, Kernprojekt Bodenmatrix: Aufnahmeanleitung zur ersten Erhebung 1994-1999* (p. 56 S.) [Application/pdf]. ETH Zurich. https://doi.org/10.3929/ETHZ-A-004375470

Wang, R., Bicharanloo, B., Shirvan, M. B., Cavagnaro, T. R., Jiang, Y., Keitel, C., & Dijkstra, F. A. (2021). A novel ^{13}C pulse-labelling method to quantify the contribution of rhizodeposits to soil respiration in a grassland exposed to drought and nitrogen addition. *New Phytologist*, *230*(2), 857–866. https://doi.org/10.1111/nph.17118

Wang, Y., Amundson, R., & Niu, X. (2000). Seasonal and altitudinal variation in decomposition of soil organic matter inferred from radiocarbon measurements of soil CO_2 flux. *Global Biogeochemical Cycles*, *14*(1), 199–211. https://doi.org/10.1029/1999GB900074

Wang, Y., Paul, S. M., Jocher, M., Espic, C., Alewell, C., Szidat, S., & Leifeld, J. (2021). Soil carbon loss from drained agricultural peatland after coverage with mineral soil. *Science of The Total Environment*, *800*, 149498. https://doi.org/10.1016/j.scitotenv.2021.149498

Werth, M., & Kuzyakov, Y. (2008). Root-derived carbon in soil respiration and microbial biomass determined by 14C and 13C. *Soil Biology and Biochemistry*, *40*(3), 625–637. https://doi.org/10.1016/j.soilbio.2007.09.022

Wunderlich, S., & Borken, W. (2012). Partitioning of soil CO₂ efflux in un-manipulated and experimentally flooded plots of a temperate fen. *Biogeosciences*, *9*(8), 3477–3489. https://doi.org/10.5194/bg-9-3477-2012

Wüst-Galley, C., Grünig, A., & Leifeld, J. (2020). Land use-driven historical soil carbon losses in Swiss peatlands. *Landscape Ecology*, *35*(1), 173–187. https://doi.org/10.1007/s10980-019-00941-5

Xiao, H. B., Shi, Z. H., Li, Z. W., Chen, J., Huang, B., Yue, Z. J., & Zhan, Y. M. (2021). The regulatory effects of biotic and abiotic factors on soil respiration under different land-use types. *Ecological Indicators*, *127*, 107787. https://doi.org/10.1016/j.ecolind.2021.107787

Zanella, A., Jabiol, B., Ponge, J.-F., & Sartori, G. (2011). *European Humus Forms Reference Base*. https://hal.science/hal-00541496v2

Zhang, D., Hui, D., Luo, Y., & Zhou, G. (2008). Rates of litter decomposition in terrestrial ecosystems: Global patterns and controlling factors. *Journal of Plant Ecology*, *1*(2), 85–93. https://doi.org/10.1093/jpe/rtn002

Zhou, X., Wan, S., & Luo, Y. (2007). Source components and interannual variability of soil CO_2 efflux under experimental warming and clipping in a grassland ecosystem. *Global Change Biology*, *13*(4), 761–775. https://doi.org/10.1111/j.1365-2486.2007.01333.x